

Nonlinear Traffic Prediction as a Matrix Completion Problem with Ensemble Learning

Wenqing Li¹, Chuhan Yang², and Saif Eddin Jabari^{*1,2}

¹New York University Abu Dhabi, Saadiyat Island, P.O. Box 129188, Abu Dhabi, U.A.E.

²New York University Tandon School of Engineering, Brooklyn NY

Abstract

We focus on short-term traffic forecasting for traffic operations management. Specifically, we focus on forecasting traffic network sensor states in high-resolution (second-by-second). Most work on traffic forecasting has focused on predicting aggregated traffic variables, typically over intervals that are no shorter than 5 minutes. The data resolution required for traffic operations is challenging since high-resolution data exhibit heavier oscillations and precise patterns are harder to capture. We propose a (big) data driven methodology for this purpose. Our contributions can be summarized as offering three major insights: first, we show how the forecasting problem can be modeled as a matrix completion problem. Second, we employ a block-coordinate descent algorithm and demonstrate that the algorithm converges in sub-linear time to a block coordinate-wise optimizer. This allows us to capitalize on the “bigness” of high-resolution data in a computationally feasible way. Third, we develop an adaptive boosting (or ensemble learning) approach to reduce the training error to within any arbitrary error threshold. The latter utilizes past days, so that the boosting can be interpreted as capturing periodic patterns in the data. The performance of the proposed method is analyzed theoretically and tested empirically using a real-world high-resolution traffic dataset from Abu Dhabi, UAE. Our experimental results show that the proposed method outperforms other state-of-the-art algorithms.

Keywords: Traffic prediction, high-resolution data, matrix completion, kernel regression, sparse approximation, ensemble learning, adaptive boosting.

1 Introduction

Traffic prediction is an essential component of modern intelligent transportation systems (ITS). It assists system operators in scheduling interventions and helps provide travelers with route guidance. Traffic prediction tools in the literature almost exclusively use aggregated data (e.g., 5-15 minutes). While relative success has been reported on the low-resolution front, these methods do not offer sufficient accuracy for traffic operations applications, which operate on a much finer time cadence.

The increasing availability of high-resolution data presents an opportunity to re-think prediction techniques for traffic operations in general but specifically for traffic signal systems. For example, the SMART-Signal system [31] records every time a vehicle is detected (arrival and departure times to sensors) and every signal change event. Such valuable information should be leveraged for traffic operations purposes.

Existing data analysis methods are either model-based or data-driven. Techniques that are geared

towards the estimation of traffic densities or speeds from both fixed and mobile sensors are examples of the former [15, 16, 18, 19, 33, 40–42, 44, 57, 59]. Data-driven techniques are becoming more popular with the increasing availability of traffic data. For traffic prediction and forecasting, data-driven methodologies fall in one of two major categories: parametric approaches and non-parametric approaches. Time series models dominate the category of parametric techniques. For example, autoregressive integrated moving average (ARIMA) [4, 26–28, 47, 54] and vector variants (VARIMA) [9, 22–24, 46] have been widely used and demonstrated to be successful. These models assume a parametric linear relationship between the label and a finite number of past states of the label itself. Their major limitation is that they tend to focus on reproducing mean patterns and fail to capture rapid fluctuation in the data. This implies that time series models are not suitable for high-resolution data. Non-parametric methods, on the other hand, do not assume any functional model forms and are typically data-driven. The basic idea behind non-parametric techniques is that they learn a general form from the historical data and use it to predict future data. Non-parametric methods can be divided into two types: non-parametric regression such as support vector regression (SVR) [13, 21, 55] and artificial neural networks (ANN) [25, 32, 34–36, 38]. Compared with time series models which assume that traffic data vary linearly over time, SVR and ANN techniques can capture nonlinear variations in traffic data. The advantage of SVR models is that they can learn representative features by using various kernels. For this reason, SVR has been successfully applied to predict traffic data such as flow [13, 21], headway [58], and travel time [5, 6, 17, 55]. Ma et al. [21] further proposed an online version of SVR, which can efficiently update the model when new data is added. Alternatively, ANNs are among the first non-parametric methods that have been applied to traffic prediction, and there is a wealth of literature on the subject, from simple multilayer perceptrons (MLPs) [34] to more complicated architectures as recurrent neural networks (RNNs) [25, 36, 38], convolutional neural networks (CNNs) [35] and even combinations of RNNs and CNNs [32].

Numerous studies have analyzed the relationship between data resolution and traffic prediction performance for different applications [10, 14, 39, 49–51]. A general finding is that the higher the resolution of the data, the less accurate the predictions. For example, Cheol et al. [39] state that strong variations appear when the aggregation intervals get shorter than 3 minutes. The Highway Capacity Manual [50] recommends aggregation into 15 minute time intervals. On the other hand, valuable information is lost upon aggregating data [51], which makes it harder for the models to capture reality. For this reason, Tan et al. [49] selected aggregation at the 3 minute level as a compromise between prediction quality and information loss. Vlahogianni et al. [51] suggest increasing the data resolution level for real-time adaptive control.

To summarize, recent works on traffic prediction have focused on using aggregated data, where both parametric and non-parametric models were utilized. To our best of knowledge, few works have investigated the utilization of high-resolution data for traffic prediction. Due to the complex non-linearities in traffic data, we consider a non-parametric approach and propose a novel non-parametric traffic prediction method for high-resolution data. One of the primary challenges when working with high-resolution traffic data is that the data is prone to irregular oscillation. Well-known patterns in traffic data tend to emerge when observed over longer periods. As an example, consider a time series of sensor occupancies, strings of zeros and ones: One requires a long string (which means longer periods) to determine whether the data pertain to free-flowing or congested traffic. Over a short time interval, such a sensor can (locally) change state from being unoccupied (zero traffic density) to fully occupied (jammed traffic density). The patterns of the zeros and ones can seem highly irregular and often exhibit sparsity. For example, the ones may occur in batches when the corresponding sensor is located near the downstream end of a signalized road. When the data exhibit sparsity, traditional prediction techniques tend to ignore the sparse data, treating them as outliers, or as very small but wide spikes as a result of averaging.

To this end, this paper proposes a *ensemble ma-*

trix completion formulation and block coordinate descent method for *nonlinear* traffic prediction using high-resolution data. The contributions of the proposed model are threefold: First, we present a novel formulation of traffic prediction as a matrix completion problem. Our formulation extends traditional modeling approaches (e.g., vector auto-regressive time series) in the nonlinear dependence between the labels and the inputs can be accommodated with ease. The model can be described as being *transductive* in that we leverage statistical information in the testing data (only the inputs). This, in turn, allows for a dynamic implementation that can adapt to streaming high-resolution data. We consider (and leverage), for the first time, the natural sparsity and “bigness” of high-resolution traffic data, in a way that is intrinsic to our formulation. Second, we develop block coordinate descent technique to solve the proposed matrix completion problems and analytically demonstrate that the algorithm converges to a block coordinate-wise minimizer (or Nash point). We also demonstrate analytically that the convergence rate is sub-linear, meaning that each iteration (which only involves a series of algebraic manipulation) produces an order of magnitude reduction in the distance from optimality. This means that only few iterations are required to solve the problem, allowing for real-time implementation. Third, the performance of the model is further boosted by forming an ensemble of matrix completion problems using datasets from past days. The merits are twofold: training errors can be reduced to arbitrarily small numbers while capturing and exploiting trends in the data from past days. This also offers interpretability that is usually sacrificed with most large-scale machine learning tools (e.g., deep neural nets).

The remainder of this paper is organized as follows: Sec. 2 formulates the traffic prediction problem as a matrix completion problem. The block-coordinate descent algorithm is presented in Sec. 3 along with all convergence results. Sec. 4 develops the ensemble learning extension, presents an analysis of the training error, and presents a time complexity analysis of the overall proposed approach. We present our empirical tests in Sec. 5 and conclude the paper in Sec. 6.

2 Traffic Prediction as a Matrix Completion Problem: Problem Formulation

2.1 Notation and Preliminaries

The task of traffic prediction is to learn a mapping between the output space of the predicted data (future data) and the input space of predictors (recent data). Let $\mathbf{x}(t) \in \{0, 1\}^n$ represent a set of n network detector states at time $t \in \mathbb{Z}_+$; an element of the vector $\mathbf{x}(t)$ is 0 if the corresponding detector is unoccupied at time t and is equal to 1, otherwise. We consider as input at time step t the present detector state, and previous states up to a lag of size L . The parameter L depends on temporal correlations in the data, and has been comprehensively discussed in previous work, e.g., [52]. We represent this input at time t by applying a backshift operator up to order L , $B_L : \mathbb{R}^n \rightarrow \mathbb{R}^{nL}$, which is given by

$$B_L \mathbf{x}(t) = \begin{bmatrix} \mathbf{x}(t - L + 1) \\ \vdots \\ \mathbf{x}(t) \end{bmatrix}. \quad (1)$$

The output of the prediction, performed at time t , which we denote by $\mathbf{y}(t) \in \mathbb{R}^n$, is simply the state of the n network detectors at some prediction horizon $H \in \mathbb{Z}_+$ time steps later, that is $\mathbf{y}(t) = \mathbf{x}(t + H)$. Let T_{tr} denote the number of training samples. The inputs in the training sample cover the interval $t \in \{1, \dots, T_{\text{tr}}\}$, which we denote by $\{B_L \mathbf{x}_{\text{tr}}(t), \mathbf{y}_{\text{tr}}(t)\}_{t=1}^{T_{\text{tr}}}$. As in (1)

$$B_L \mathbf{x}_{\text{tr}}(t) = \begin{bmatrix} \mathbf{x}_{\text{tr}}(t - L + 1) \\ \vdots \\ \mathbf{x}_{\text{tr}}(t) \end{bmatrix} \quad (2)$$

is the input associated with the sample at time t and the corresponding output vector is $\mathbf{y}_{\text{tr}}(t) = \mathbf{x}_{\text{tr}}(t + H) \in \mathbb{R}^n$. The inputs and outputs at a single time step t are illustrated in Fig. 1

2.2 Traffic Prediction and Matrix Rank Minimization

Assuming a linear relationship between the input and output (which will be relaxed below), we may write

$$\mathbf{y}_{\text{tr}}(t) = \langle \mathbf{W}, B_L \mathbf{x}_{\text{tr}}(t) \rangle = \mathbf{W}^\top B_L \mathbf{x}_{\text{tr}}(t), \quad (3)$$

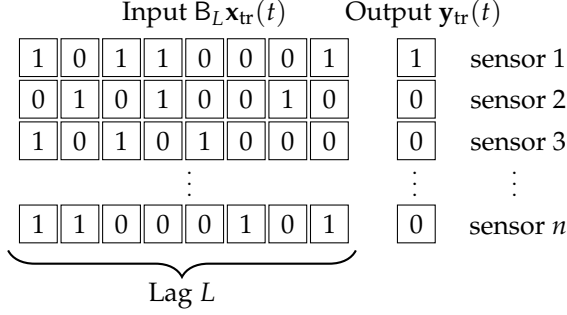


Figure 1: An Illustration of Training Inputs and Outputs at a Single Time Step.

where $\mathbf{W} \in \mathbb{R}^{n \times nL}$ is the (regression) coefficients matrix and $\langle \cdot, \cdot \rangle$ is the inner product. Let T_{te} be the number of testing samples. We denote the set of testing data over the prediction interval $t \in \{T_{tr} + 1, \dots, T_{tr} + T_{te}\}$ by $\{B_L \mathbf{x}_{te}(t), \mathbf{y}_{te}(t)\}_{t=T_{tr}+1}^{T_{tr}+T_{te}}$ and write their (linear) relationship as

$$\mathbf{y}_{te}(t) = \langle \mathbf{W}, B_L \mathbf{x}_{te}(t) \rangle = \mathbf{W}^\top B_L \mathbf{x}_{te}(t). \quad (4)$$

To set the prediction problem up as a matrix completion problem, we first define the input data matrices

$$\mathbf{X}_{tr} \equiv [B_L \mathbf{x}_{tr}(1) \quad \dots \quad B_L \mathbf{x}_{tr}(T_{tr})] \in \mathbb{R}^{nL \times T_{tr}} \quad (5)$$

and

$$\mathbf{X}_{te} \equiv [B_L \mathbf{x}_{te}(T_{tr} + 1) \quad \dots \quad B_L \mathbf{x}_{te}(T_{tr} + T_{te})] \in \mathbb{R}^{nL \times T_{te}}. \quad (6)$$

Their corresponding output matrices are defined as

$$\mathbf{Y}_{tr} \equiv [\mathbf{y}_{tr}(1) \quad \dots \quad \mathbf{y}_{tr}(T_{tr})] \in \mathbb{R}^{n \times T_{tr}} \quad (7)$$

and

$$\mathbf{Y}_{te} \equiv [\mathbf{y}_{te}(T_{tr} + 1) \quad \dots \quad \mathbf{y}_{te}(T_{tr} + T_{te})] \in \mathbb{R}^{n \times T_{te}}. \quad (8)$$

We then define *joint matrix*, which concatenates both the training and the testing data, as

$$\mathbf{Z} \equiv \begin{bmatrix} \mathbf{Y}_{tr} & \mathbf{Y}_{te} \\ \mathbf{X}_{tr} & \mathbf{X}_{te} \end{bmatrix} \in \mathbb{R}^{(n+nL) \times (T_{tr}+T_{te})}. \quad (9)$$

The entries corresponding to \mathbf{Y}_{te} in \mathbf{Z} are unknown and constitute the solution of the prediction problem. Hence the prediction problem can be cast as

a matrix completion problem. From (3) and (4), we have that

$$[\mathbf{Y}_{tr} \quad \mathbf{Y}_{te}] = \mathbf{W} [\mathbf{X}_{tr} \quad \mathbf{X}_{te}], \quad (10)$$

which implies that the joint matrix \mathbf{Z} as defined in (9) has low rank as a result of linear dependencies in the rows of \mathbf{Z} implied by (10). Thus, removing entries corresponding to \mathbf{Y}_{te} and completion of the joint matrix \mathbf{Z} via rank-minimization techniques is equivalent to directly producing predictions (and bypassing the need to estimate \mathbf{W}). The higher the linear dependence in the matrix \mathbf{Z} (represented by its rank), the more parsimonious the resulting prediction, which is a desirable feature from a statistical point of view.

2.3 Relaxing the Linearity Using Kernels

We relax the linearity assumption by mapping the inputs to a higher dimensional feature space, via kernel “basis” functions, and solve a linear prediction problem in the higher dimensional space [48]. In the training stage, the nonlinear relationship can be expressed as

$$\mathbf{y}_{tr}(t) = \langle \mathbf{W}, \phi(B_L \mathbf{x}_{tr}(t)) \rangle, \quad (11)$$

where $\phi : \mathbb{R}^{nL} \rightarrow \mathbb{R}^h$ is the nonlinear function that maps the input space to the high-dimensional feature space ($h > nL$) and with slight notation abuse $\mathbf{W} \in \mathbb{R}^{n \times h}$ is the regression matrix. Note that the inner product of \mathbf{W} and $\phi(\mathbf{x})$ can be learned using the *kernel trick* avoiding the need to compute the map ϕ ; see for example [29, 45]. Mapping functions are related to kernels via

$$K(\mathbf{x}_1, \mathbf{x}_2) = \langle \phi(\mathbf{x}_1), \phi(\mathbf{x}_2) \rangle = \phi(\mathbf{x}_1)^\top \phi(\mathbf{x}_2), \quad (12)$$

where K is a kernel (a weighted distance measure). We note that not all known kernel functions have known mapping functions (e.g., the widely used Gaussian kernels). We shall prescribe a kernel and treat the mapping function as an unknown. Specifically, we shall adopt a radial basis function with periodical patterns (RBF-P), which appends a component that captures potential periodic patterns to

traditional radial basis functions [30]:

$$\begin{aligned} K_P(\mathbf{x}_1(t_1), \mathbf{x}_2(t_2)) \\ = \exp \left(-\gamma \|\mathbf{B}_L \mathbf{x}_1(t_1) - \mathbf{B}_L \mathbf{x}_2(t_2)\|_2^2 \right. \\ \left. - \gamma_P d_P(t_1, t_2)^2 \right), \end{aligned} \quad (13)$$

where P is the period in the data (e.g., one signal cycle), γ and γ_P are weights associated with the radial basis function and the periodicity, respectively, and

$$d_P(t_1, t_2) \equiv \min \left\{ |(t_1 - t_2) \bmod P|, \right. \\ \left. P - |(t_1 - t_2) \bmod P| \right\} \quad (14)$$

is a temporal distance (modulo periodicity). The testing samples are related, similar to the training samples, as follows:

$$\mathbf{y}_{te}(t) = \langle \mathbf{W}, \phi(\mathbf{B}_L \mathbf{x}_{te}(t)) \rangle, \quad (15)$$

and the *joint matrix* in this kernelized setting is defined as:

$$\mathbf{Z} \equiv \begin{bmatrix} \mathbf{Y}_{tr} & \mathbf{Y}_{te} \\ \Phi(\mathbf{X}_{tr}) & \Phi(\mathbf{X}_{te}) \end{bmatrix} \in \mathbb{R}^{(n+h) \times (T_{tr} + T_{te})}, \quad (16)$$

where $\Phi : \mathbb{R}^{nL \times t} \rightarrow \mathbb{R}^{h \times t}$ simply applies ϕ to each column of its argument. That is

$$\Phi(\mathbf{X}_{tr}) \equiv [\phi(\mathbf{B}_L \mathbf{x}_{tr}(1)) \quad \cdots \quad \phi(\mathbf{B}_L \mathbf{x}_{tr}(T_{tr}))] \quad (17)$$

and $\Phi(\mathbf{X}_{te})$ is defined in a similar way. To further simplify notation, we define the matrices $\Phi_{tr} \equiv \Phi(\mathbf{X}_{tr}) \in \mathbb{R}^{h \times T_{tr}}$ and $\Phi_{te} \equiv \Phi(\mathbf{X}_{te}) \in \mathbb{R}^{h \times T_{te}}$. The inner products of these matrices define the kernels that we will use below. For example we define the kernel $\mathbf{K}_{tr,te}$ as:

$$\mathbf{K}_{tr,te} \equiv \langle \Phi(\mathbf{X}_{tr}), \Phi(\mathbf{X}_{te}) \rangle = \begin{bmatrix} K_P(\mathbf{x}_{tr}(1), \mathbf{x}_{te}(T_{tr})) & \cdots & K_P(\mathbf{x}_{tr}(1), \mathbf{x}_{te}(T_{tr} + T_{te})) \\ \vdots & \ddots & \vdots \\ K_P(\mathbf{x}_{tr}(T_{tr}), \mathbf{x}_{te}(T_{tr})) & \cdots & K_P(\mathbf{x}_{tr}(T_{tr}), \mathbf{x}_{te}(T_{tr} + T_{te})) \end{bmatrix}. \quad (18)$$

From (11) and (15), we have that

$$\begin{bmatrix} \mathbf{Y}_{tr} & \mathbf{Y}_{te} \end{bmatrix} = \mathbf{W} \begin{bmatrix} \phi(\mathbf{X}_{tr}) & \phi(\mathbf{X}_{te}) \end{bmatrix}, \quad (19)$$

which (again) implies that \mathbf{Z} is a low-rank matrix and that the prediction problem can be formulated as a low-rank matrix completion problem.

2.4 The Matrix Completion Problem

Our matrix completion problem seeks to find a low-rank approximation $\hat{\mathbf{Z}}$ of the matrix \mathbf{Z} . Let $\mathbb{P}_\Omega : \mathbb{R}^{p \times q} \rightarrow \mathbb{R}^{p \times q}$ be a binary mask operator:

$$[\mathbb{P}_\Omega(\mathbf{M})]_{ij} = \mathbb{1}\{(i, j) \in \Omega\} \mathbf{M}_{ij}, \quad (20)$$

where $\mathbb{1}\{(i, j) \in \Omega\}$ is the indicator function, taking the value 1 if the condition $(i, j) \in \Omega$ is true and 0 otherwise. We utilize the binary mask to exclude the output testing matrix from \mathbf{Z} . That is, we define Ω as the set of indices corresponding to non-testing

outputs, that is

$$\begin{aligned} \Omega \equiv \{ (i, j) : 1 \leq i \leq n + h, 1 \leq j \leq T_{tr} \} \cup \{ (i, j) : \\ n + 1 \leq i \leq n + h, T_{tr} + 1 \leq j \leq T_{tr} + T_{te} \}. \end{aligned} \quad (21)$$

Consequently,

$$\mathbb{P}_\Omega(\mathbf{Z}) = \begin{bmatrix} \mathbf{Y}_{tr} & \mathbf{0} \\ \Phi(\mathbf{X}_{tr}) & \Phi(\mathbf{X}_{te}) \end{bmatrix}. \quad (22)$$

The matrix completion problem is then formulated as a rank minimization problem:

$$\hat{\mathbf{Z}} \equiv \arg \min_{\mathbf{M} \in \mathbb{R}^{(n+h) \times (T_{tr} + T_{te})}} \{ \text{rank}(\mathbf{M}) : \mathbb{P}_\Omega(\mathbf{M} - \mathbf{Z}) = \mathbf{0} \}. \quad (23)$$

The solution $\hat{\mathbf{Z}}$ is interpreted as the lowest-rank matrix that matches \mathbf{Z} exactly (via the constraint) in the entries corresponding to the training data, \mathbf{Y}_{tr} and $\Phi(\mathbf{X}_{tr})$, and the input testing data, $\Phi(\mathbf{X}_{te})$. Rank minimization (23) is generally NP-hard but it was demonstrated in [2] that (23) can be solved exactly if certain sparsity conditions on \mathbf{Z} hold, by using convex optimization techniques (via convex relaxation

of the rank objective as shown below). The sparsity condition required is that \mathbf{Z} be *sufficiently incoherent*, which is achieved when the number of observed entries in the matrix, $|\Omega|$ is $O(N^{1.2}\text{rank}(\mathbf{Z})\log N)$, where $N \equiv \max\{n+h, T_{\text{tr}}+T_{\text{te}}\}$ in our context. This ensures faithful reconstruction. In our context such bounds can be easily ensured by simply using past days and longer lags (if necessary). A more useful application of this bound is to produce upper bound estimates of the rank of $\hat{\mathbf{Z}}$, which will be needed to set up the problem (25) below. Henceforth, we will focus on solving a convex relaxation of the problem and refer readers to [2, 3] for further information on these bounds.

The main difficulty lies in minimizing the matrix rank. This can be observed by noting that $\text{rank}(\mathbf{M}) = \|\sigma(\mathbf{M})\|_0$, where $\sigma(\mathbf{M})$ is a vector of the singular values of \mathbf{M} and $\|\cdot\|_0$ is the ℓ_0 pseudo-norm which counts the number of non-zero elements of its argument. We relax the objective function via a convex surrogate using the nuclear norm $\|\mathbf{M}\|_* = \text{trace}(\sqrt{\mathbf{M}^\top \mathbf{M}}) = \|\sigma(\mathbf{M})\|_1$. (The ℓ_1 norm in this context is simply the sum of the singular values, since the singular values of a matrix are always non-negative.) This yields the relaxed problem:

$$\hat{\mathbf{Z}} \equiv \arg \min_{\mathbf{M} \in \mathbb{R}^{(n+h) \times (T_{\text{tr}}+T_{\text{te}})}} \{\|\mathbf{M}\|_* : \mathbb{P}_\Omega(\mathbf{M} - \mathbf{Z}) = \mathbf{0}\}, \quad (24)$$

which is equivalent to the quadratic optimization problem [43, Lemma 5.1]

$$\begin{aligned} & \{\hat{\mathbf{U}}, \hat{\mathbf{V}}\} \\ & \equiv \arg \min_{\substack{\mathbf{U} \in \mathbb{R}^{(n+h) \times r}, \\ \mathbf{V} \in \mathbb{R}^{(T_{\text{tr}}+T_{\text{te}}) \times r}}} \{\|\mathbf{U}\|_{\text{F}}^2 + \|\mathbf{V}\|_{\text{F}}^2 : \mathbb{P}_\Omega(\mathbf{U}\mathbf{V}^\top - \mathbf{Z}) = \mathbf{0}\}, \end{aligned} \quad (25)$$

where $\|\cdot\|_{\text{F}}$ is the Frobenius norm and r is chosen so that $r \geq \text{rank}(\hat{\mathbf{Z}})$. The latter formulation utilizes a bi-linear representation $\mathbf{M} = \mathbf{U}\mathbf{V}^\top$ of the joint matrix and can be solved efficiently using alternating minimization techniques [20], an instance of which we shall develop in the next section. The latter formulation (25) can be expressed as an unconstrained

optimization problem via the Lagrangian:

$$\begin{aligned} \{\hat{\mathbf{U}}, \hat{\mathbf{V}}\} \equiv & \arg \min_{\substack{\mathbf{U} \in \mathbb{R}^{(n+h) \times r}, \\ \mathbf{V} \in \mathbb{R}^{(T_{\text{tr}}+T_{\text{te}}) \times r}}} \|\mathbb{P}_\Omega(\mathbf{U}\mathbf{V}^\top - \mathbf{Z})\|_{\text{F}}^2 \\ & + \mu(\|\mathbf{U}\|_{\text{F}}^2 + \|\mathbf{V}\|_{\text{F}}^2), \end{aligned} \quad (26)$$

where $\mu > 0$ is a Lagrange multiplier.

Another simplification can be achieved by dividing each of the two matrices \mathbf{U} and \mathbf{V} into two blocks, a training block and a testing block:

$$\mathbf{U} = \begin{bmatrix} \mathbf{U}_{\text{tr}} \\ \mathbf{U}_{\text{te}} \end{bmatrix} \text{ and } \mathbf{V} = \begin{bmatrix} \mathbf{V}_{\text{tr}} \\ \mathbf{V}_{\text{te}} \end{bmatrix}, \quad (27)$$

where $\mathbf{U}_{\text{tr}} \in \mathbb{R}^{n \times r}$, $\mathbf{V}_{\text{tr}} \in \mathbb{R}^{T_{\text{tr}} \times r}$, $\mathbf{U}_{\text{te}} \in \mathbb{R}^{h \times r}$, and $\mathbf{V}_{\text{te}} \in \mathbb{R}^{T_{\text{te}} \times r}$. This decomposition allows us to bypass use of the binary mask \mathbb{P}_Ω , simplifying the formulation further. We obtain the following optimization problem:

$$\begin{aligned} \{\hat{\mathbf{U}}_{\text{tr}}, \hat{\mathbf{U}}_{\text{te}}, \hat{\mathbf{V}}_{\text{tr}}, \hat{\mathbf{V}}_{\text{te}}\} \equiv & \arg \min_{\mathbf{U}_{\text{tr}}, \mathbf{U}_{\text{te}}, \mathbf{V}_{\text{tr}}, \mathbf{V}_{\text{te}}} \|\mathbf{U}_{\text{tr}}\mathbf{V}_{\text{tr}}^\top - \mathbf{Y}_{\text{tr}}\|_{\text{F}}^2 \\ & + \|\mathbf{U}_{\text{te}}\mathbf{V}_{\text{tr}}^\top - \Phi_{\text{tr}}\|_{\text{F}}^2 + \|\mathbf{U}_{\text{te}}\mathbf{V}_{\text{te}}^\top - \Phi_{\text{te}}\|_{\text{F}}^2 \\ & + \mu(\|\mathbf{U}_{\text{tr}}\|_{\text{F}}^2 + \|\mathbf{U}_{\text{te}}\|_{\text{F}}^2 + \|\mathbf{V}_{\text{tr}}\|_{\text{F}}^2 + \|\mathbf{V}_{\text{te}}\|_{\text{F}}^2). \end{aligned} \quad (28)$$

Again, we do not prescribe the mapping functions, but shall prescribe kernels. For this purpose, we define $\mathbf{K}_{\text{tr}, \text{tr}} \equiv \langle \Phi_{\text{tr}}, \Phi_{\text{tr}} \rangle = \Phi_{\text{tr}}^\top \Phi_{\text{tr}}$, $\mathbf{K}_{\text{tr}, \text{te}} \equiv \langle \Phi_{\text{tr}}, \Phi_{\text{te}} \rangle = \Phi_{\text{tr}}^\top \Phi_{\text{te}}$, $\mathbf{K}_{\text{te}, \text{tr}} \equiv \langle \Phi_{\text{te}}, \Phi_{\text{tr}} \rangle = \Phi_{\text{te}}^\top \Phi_{\text{tr}}$, and $\mathbf{K}_{\text{te}, \text{te}} \equiv \langle \Phi_{\text{te}}, \Phi_{\text{te}} \rangle = \Phi_{\text{te}}^\top \Phi_{\text{te}}$.

To summarize, the key features of the proposed formulation (28), as they relate to traffic prediction, are:

1. The formulation inherits all the merits of conventional *vector* time series prediction methods, namely, vector auto-regressive models (VARs) [9, 46]. Specifically, our approach is capable of capturing and leveraging spatio-temporal dependencies.
2. The use of kernels allows us to capture nonlinearities (not possible with the VAR models in the literature), which one expects to see in traffic flow patterns, particularly in high-resolution traffic data.
3. The prediction results can be directly obtained without computing regression parameters. This is a particularly desirable feature for

real-time implementations, where the parameters change throughout the day, from day-to-day, and throughout the year (seasonal effects).

Mathematically, the matrix completion problem (28) is not (in general) convex in all of its block coordinates $\{\mathbf{U}_{\text{tr}}, \mathbf{U}_{\text{te}}, \mathbf{V}_{\text{tr}}, \mathbf{V}_{\text{te}}\}$ simultaneously but it is convex in each of the blocks separately. (For intuition, readers may consider –as an exercise– convexity of the function $f(x, y) = (xy - 1)^2$). Such problems are referred to as *block multi-convex* [56]. Let $F(\mathbf{U}_{\text{tr}}, \mathbf{U}_{\text{te}}, \mathbf{V}_{\text{tr}}, \mathbf{V}_{\text{te}})$ denote the objective function in (28):

$$\begin{aligned} F(\mathbf{U}_{\text{tr}}, \mathbf{U}_{\text{te}}, \mathbf{V}_{\text{tr}}, \mathbf{V}_{\text{te}}) &\equiv \|\mathbf{U}_{\text{tr}} \mathbf{V}_{\text{tr}}^\top - \mathbf{Y}_{\text{tr}}\|_{\text{F}}^2 \\ &\quad + \|\mathbf{U}_{\text{te}} \mathbf{V}_{\text{te}}^\top - \Phi_{\text{tr}}\|_{\text{F}}^2 + \|\mathbf{U}_{\text{te}} \mathbf{V}_{\text{te}}^\top - \Phi_{\text{te}}\|_{\text{F}}^2 \\ &\quad + \mu(\|\mathbf{U}_{\text{tr}}\|_{\text{F}}^2 + \|\mathbf{U}_{\text{te}}\|_{\text{F}}^2 + \|\mathbf{V}_{\text{tr}}\|_{\text{F}}^2 + \|\mathbf{V}_{\text{te}}\|_{\text{F}}^2). \end{aligned} \quad (29)$$

We seek a solution $\{\bar{\mathbf{U}}_{\text{tr}}, \bar{\mathbf{U}}_{\text{te}}, \bar{\mathbf{V}}_{\text{tr}}, \bar{\mathbf{V}}_{\text{te}}\}$ for which the following variational inequalities hold for all $\mathbf{U}_{\text{tr}} \in \mathbb{R}^{n \times r}$, all $\mathbf{U}_{\text{te}} \in \mathbb{R}^{h \times r}$, all $\mathbf{V}_{\text{tr}} \in \mathbb{R}^{T_{\text{tr}} \times r}$, and all $\mathbf{V}_{\text{te}} \in \mathbb{R}^{T_{\text{te}} \times r}$:

$$\langle \partial_{\mathbf{U}_{\text{tr}}} F(\bar{\mathbf{U}}_{\text{tr}}, \bar{\mathbf{U}}_{\text{te}}, \bar{\mathbf{V}}_{\text{tr}}, \bar{\mathbf{V}}_{\text{te}}), \mathbf{U}_{\text{tr}} - \bar{\mathbf{U}}_{\text{tr}} \rangle \geq 0, \quad (30)$$

$$\langle \partial_{\mathbf{U}_{\text{te}}} F(\bar{\mathbf{U}}_{\text{tr}}, \bar{\mathbf{U}}_{\text{te}}, \bar{\mathbf{V}}_{\text{tr}}, \bar{\mathbf{V}}_{\text{te}}), \mathbf{U}_{\text{te}} - \bar{\mathbf{U}}_{\text{te}} \rangle \geq 0, \quad (31)$$

$$\langle \partial_{\mathbf{V}_{\text{tr}}} F(\bar{\mathbf{U}}_{\text{tr}}, \bar{\mathbf{U}}_{\text{te}}, \bar{\mathbf{V}}_{\text{tr}}, \bar{\mathbf{V}}_{\text{te}}), \mathbf{V}_{\text{tr}} - \bar{\mathbf{V}}_{\text{tr}} \rangle \geq 0, \quad (32)$$

and

$$\langle \partial_{\mathbf{V}_{\text{te}}} F(\bar{\mathbf{U}}_{\text{tr}}, \bar{\mathbf{U}}_{\text{te}}, \bar{\mathbf{V}}_{\text{tr}}, \bar{\mathbf{V}}_{\text{te}}), \mathbf{V}_{\text{te}} - \bar{\mathbf{V}}_{\text{te}} \rangle \geq 0, \quad (33)$$

where $\partial_{\mathbf{U}}$ denotes the partial derivative operator with respect to the matrix \mathbf{U} . This type of solution is referred to as a *block coordinate-wise minimizer* or a *Nash point* in the sense that one cannot further minimize F by changing any of the four block coordinates separately.

3 Block Coordinate Descent Algorithm

3.1 Block Coordinate Descent and Thresholding

The proposed block coordinate descent algorithm first updates the two \mathbf{U} blocks, \mathbf{U}_{tr} and \mathbf{U}_{te} , and then

updates the two \mathbf{V} blocks, \mathbf{V}_{tr} and \mathbf{V}_{te} . The objective functions of the four sub-problems in iteration k are stated as

$$F_1^{[k]}(\mathbf{U}_{\text{tr}}) \equiv \|\mathbf{U}_{\text{tr}} \hat{\mathbf{V}}_{\text{tr}}^{[k-1]\top} - \mathbf{Y}_{\text{tr}}\|_{\text{F}}^2 + 2\mu\|\mathbf{U}_{\text{tr}}\|_{\text{F}}^2, \quad (34)$$

$$\begin{aligned} F_2^{[k]}(\mathbf{U}_{\text{te}}) &\equiv \|\mathbf{U}_{\text{te}} \hat{\mathbf{V}}_{\text{tr}}^{[k-1]\top} - \Phi_{\text{tr}}\|_{\text{F}}^2 \\ &\quad + \|\mathbf{U}_{\text{te}} \hat{\mathbf{V}}_{\text{te}}^{[k-1]\top} - \Phi_{\text{te}}\|_{\text{F}}^2 + 2\mu\|\mathbf{U}_{\text{te}}\|_{\text{F}}^2, \end{aligned} \quad (35)$$

$$\begin{aligned} F_3^{[k]}(\mathbf{V}_{\text{tr}}) &\equiv \|\hat{\mathbf{U}}_{\text{tr}}^{[k]} \mathbf{V}_{\text{tr}}^\top - \mathbf{Y}_{\text{tr}}\|_{\text{F}}^2 \\ &\quad + \|\hat{\mathbf{U}}_{\text{te}}^{[k]} \mathbf{V}_{\text{tr}}^\top - \Phi_{\text{tr}}\|_{\text{F}}^2 + 2\mu\|\mathbf{V}_{\text{tr}}\|_{\text{F}}^2, \end{aligned} \quad (36)$$

and

$$F_4^{[k]}(\mathbf{V}_{\text{te}}) \equiv \|\hat{\mathbf{U}}_{\text{te}}^{[k]} \mathbf{V}_{\text{te}}^\top - \Phi_{\text{te}}\|_{\text{F}}^2 + 2\mu\|\mathbf{V}_{\text{te}}\|_{\text{F}}^2. \quad (37)$$

The factors of two in the regularizers are unnecessary but we use them here to reduce clutter latter on. The updates are obtained in closed form; the updated \mathbf{U} blocks are given by:

$$\begin{aligned} \hat{\mathbf{U}}_{\text{tr}}^{[k]} &= \arg \min_{\mathbf{U}_{\text{tr}} \in \mathbb{R}^{n \times r}} F_1^{[k]}(\mathbf{U}_{\text{tr}}) \\ &= \mathbf{Y}_{\text{tr}} \hat{\mathbf{V}}_{\text{tr}}^{[k-1]} (\hat{\mathbf{V}}_{\text{tr}}^{[k-1]\top} \hat{\mathbf{V}}_{\text{tr}}^{[k-1]} + 2\mu\mathbf{I})^{-1} \end{aligned} \quad (38)$$

and

$$\begin{aligned} \hat{\mathbf{U}}_{\text{te}}^{[k]} &= \arg \min_{\mathbf{U}_{\text{te}} \in \mathbb{R}^{h \times r}} F_2^{[k]}(\mathbf{U}_{\text{te}}) = (\Phi_{\text{tr}} \hat{\mathbf{V}}_{\text{tr}}^{[k-1]} + \Phi_{\text{te}} \hat{\mathbf{V}}_{\text{te}}^{[k-1]}) \\ &\quad \times (\hat{\mathbf{V}}_{\text{tr}}^{[k-1]\top} \hat{\mathbf{V}}_{\text{tr}}^{[k-1]} + \hat{\mathbf{V}}_{\text{te}}^{[k-1]\top} \hat{\mathbf{V}}_{\text{te}}^{[k-1]} + 2\mu\mathbf{I})^{-1}. \end{aligned} \quad (39)$$

The updated \mathbf{V} blocks are then given by:

$$\begin{aligned} \hat{\mathbf{V}}_{\text{tr}}^{[k]} &= \arg \min_{\mathbf{V}_{\text{tr}} \in \mathbb{R}^{T_{\text{tr}} \times r}} F_3^{[k]}(\mathbf{V}_{\text{tr}}) = (\mathbf{Y}_{\text{tr}}^\top \hat{\mathbf{U}}_{\text{tr}}^{[k]} + \Phi_{\text{tr}}^\top \hat{\mathbf{U}}_{\text{te}}^{[k]}) \\ &\quad \times (\hat{\mathbf{U}}_{\text{te}}^{[k]\top} \hat{\mathbf{U}}_{\text{te}}^{[k]} + \hat{\mathbf{U}}_{\text{tr}}^{[k]\top} \hat{\mathbf{U}}_{\text{tr}}^{[k]} + 2\mu\mathbf{I})^{-1} \end{aligned} \quad (40)$$

and

$$\begin{aligned} \hat{\mathbf{V}}_{\text{te}}^{[k]} &= \arg \min_{\mathbf{V}_{\text{te}} \in \mathbb{R}^{T_{\text{te}} \times r}} F_4^{[k]}(\mathbf{V}_{\text{te}}) \\ &= \Phi_{\text{te}}^\top \hat{\mathbf{U}}_{\text{te}}^{[k]} (\hat{\mathbf{U}}_{\text{te}}^{[k]\top} \hat{\mathbf{U}}_{\text{te}}^{[k]} + 2\mu\mathbf{I})^{-1}. \end{aligned} \quad (41)$$

Since Φ_{tr} and Φ_{te} are unknown, $\hat{\mathbf{U}}_{\text{te}}^{[k]}$ cannot be calculated explicitly. However, this calculation is not required to produce a prediction: $\hat{\mathbf{Y}}_{\text{te}} \equiv \hat{\mathbf{U}}_{\text{tr}} \hat{\mathbf{V}}_{\text{te}}^\top$. To

produce this estimate, in each iteration k we need to be able to calculate $\hat{\mathbf{U}}_{\text{tr}}^{[k]}$ and $\hat{\mathbf{V}}_{\text{te}}^{[k]\top}$. To calculate these quantities, we need (i) $\hat{\mathbf{V}}_{\text{tr}}^{[k-1]}$, (ii) $\Phi_{\text{te}}^\top \hat{\mathbf{U}}_{\text{te}}^{[k]}$, and (iii) $\hat{\mathbf{U}}_{\text{te}}^{[k]\top} \hat{\mathbf{U}}_{\text{te}}^{[k]}$. We start with (iii): assuming that all required calculations have been performed for iteration $k-1$, we have from (39) that

$$\begin{aligned} \hat{\mathbf{U}}_{\text{te}}^{[k]\top} \hat{\mathbf{U}}_{\text{te}}^{[k]} &= (\hat{\mathbf{V}}_{\text{tr}}^{[k-1]\top} \hat{\mathbf{V}}_{\text{tr}}^{[k-1]} + \hat{\mathbf{V}}_{\text{te}}^{[k-1]\top} \hat{\mathbf{V}}_{\text{te}}^{[k-1]} + \mu \mathbf{I})^{-1} \\ &\quad \times \left(\hat{\mathbf{V}}_{\text{tr}}^{[k-1]\top} \mathbf{K}_{\text{tr,tr}} \hat{\mathbf{V}}_{\text{tr}}^{[k-1]} + \hat{\mathbf{V}}_{\text{te}}^{[k-1]\top} \mathbf{K}_{\text{te,tr}} \hat{\mathbf{V}}_{\text{tr}}^{[k-1]} \right. \\ &\quad \left. + \hat{\mathbf{V}}_{\text{tr}}^{[k-1]\top} \mathbf{K}_{\text{tr,te}} \hat{\mathbf{V}}_{\text{te}}^{[k-1]} + \hat{\mathbf{V}}_{\text{te}}^{[k-1]\top} \mathbf{K}_{\text{te,te}} \hat{\mathbf{V}}_{\text{te}}^{[k-1]} \right) \\ &\quad \times (\hat{\mathbf{V}}_{\text{tr}}^{[k-1]\top} \hat{\mathbf{V}}_{\text{tr}}^{[k-1]} + \hat{\mathbf{V}}_{\text{te}}^{[k-1]\top} \hat{\mathbf{V}}_{\text{te}}^{[k-1]} + \mu \mathbf{I})^{-1}, \quad (42) \end{aligned}$$

which only involves known quantities. Similarly, for (ii) we have from (39) that

$$\begin{aligned} \Phi_{\text{te}}^\top \hat{\mathbf{U}}_{\text{te}}^{[k]} &= (\mathbf{K}_{\text{te,tr}} \hat{\mathbf{V}}_{\text{tr}}^{[k-1]} + \mathbf{K}_{\text{te,te}} \hat{\mathbf{V}}_{\text{te}}^{[k-1]}) \\ &\quad \times (\hat{\mathbf{V}}_{\text{tr}}^{[k-1]\top} \hat{\mathbf{V}}_{\text{tr}}^{[k-1]} + \hat{\mathbf{V}}_{\text{te}}^{[k-1]\top} \hat{\mathbf{V}}_{\text{te}}^{[k-1]} + \mu \mathbf{I})^{-1}, \quad (43) \end{aligned}$$

which also only involves known quantities. For (i), we need to be able to calculate $\Phi_{\text{tr}}^\top \hat{\mathbf{U}}_{\text{te}}^{[k-1]}$ and $\hat{\mathbf{U}}_{\text{te}}^{[k-1]\top} \hat{\mathbf{U}}_{\text{te}}^{[k-1]}$. These quantities also only involve known quantities; they are the same as (43) and (42), respectively (since k is arbitrary). Note that this also allows for calculating training estimates $\hat{\mathbf{Y}}_{\text{tr}}^{[k]} \equiv \hat{\mathbf{U}}_{\text{tr}}^{[k]} \hat{\mathbf{V}}_{\text{tr}}^{[k]\top}$ in each iteration, which we will need in our ensemble approach presented below. The steps involved in performing a single update are summarized in Alg. 1.

Soft thresholding: The predictions $\hat{\mathbf{Y}}$ produced by Algorithm 1 will produce values that are not necessarily restricted to $\{0,1\}$. It is standard practice is to employ thresholding as a post-processing step in classification and prediction problems, e.g., in neural networks [37] and logistic regression based methods [11] to project non-binary solutions to binary values. The algorithm employed for thresholding in this paper is given in Algorithm 2. Our thresholding procedure can simply be described as one that produces cut-offs for each of the n network sensors separately. The algorithm chooses cut-offs, denoted $\{\tau_j\}_{j=1}^n$ that result in the lowest training error.

Algorithm 1: Block Coordinate Descent

Data: $\mathbf{Y}_{\text{tr}}, \mathbf{K}_{\text{tr,tr}}, \mathbf{K}_{\text{tr,te}}, \mathbf{K}_{\text{te,tr}}, \mathbf{K}_{\text{te,te}}, \hat{\mathbf{U}}_{\text{tr}}^{[0]}, \hat{\mathbf{V}}_{\text{tr}}^{[0]}, \hat{\mathbf{V}}_{\text{te}}^{[0]}$
Result: $\hat{\mathbf{Y}}_{\text{tr}}, \hat{\mathbf{Y}}_{\text{te}}$

```

1 Initialize:  $k \leftarrow 1$ 
2 while stopping criterion not met do
3    $\hat{\mathbf{U}}_{\text{tr}}^{[k]} \leftarrow \mathbf{Y}_{\text{tr}} \hat{\mathbf{V}}_{\text{tr}}^{[k-1]} (\hat{\mathbf{V}}_{\text{tr}}^{[k-1]\top} \hat{\mathbf{V}}_{\text{tr}}^{[k-1]} + 2\mu \mathbf{I})^{-1}$ 
4    $\mathbf{C}_1 \leftarrow (\hat{\mathbf{V}}_{\text{tr}}^{[k-1]\top} \hat{\mathbf{V}}_{\text{tr}}^{[k-1]} + \hat{\mathbf{V}}_{\text{te}}^{[k-1]\top} \hat{\mathbf{V}}_{\text{te}}^{[k-1]} + 2\mu \mathbf{I})^{-1}$ 
5    $\mathbf{C}_2 \leftarrow \hat{\mathbf{V}}_{\text{tr}}^{[k-1]\top} \mathbf{K}_{\text{tr,tr}} \hat{\mathbf{V}}_{\text{tr}}^{[k-1]} + \hat{\mathbf{V}}_{\text{te}}^{[k-1]\top} \mathbf{K}_{\text{te,tr}} \hat{\mathbf{V}}_{\text{tr}}^{[k-1]}$ 
6    $\mathbf{C}_3 \leftarrow \hat{\mathbf{V}}_{\text{tr}}^{[k-1]\top} \mathbf{K}_{\text{tr,te}} \hat{\mathbf{V}}_{\text{te}}^{[k-1]} + \hat{\mathbf{V}}_{\text{te}}^{[k-1]\top} \mathbf{K}_{\text{te,te}} \hat{\mathbf{V}}_{\text{te}}^{[k-1]}$ 
7    $\Phi_{\text{te}}^\top \hat{\mathbf{U}}_{\text{te}}^{[k]} \leftarrow (\mathbf{K}_{\text{te,tr}} \hat{\mathbf{V}}_{\text{tr}}^{[k-1]} + \mathbf{K}_{\text{te,te}} \hat{\mathbf{V}}_{\text{te}}^{[k-1]}) \mathbf{C}_1$ 
8    $\hat{\mathbf{U}}_{\text{te}}^{[k]\top} \hat{\mathbf{U}}_{\text{te}}^{[k]} \leftarrow \mathbf{C}_1 (\mathbf{C}_2 + \mathbf{C}_3) \mathbf{C}_1$ 
9    $\mathbf{C}_4 \leftarrow (\hat{\mathbf{U}}_{\text{te}}^{[k]\top} \hat{\mathbf{U}}_{\text{te}}^{[k]} + \hat{\mathbf{U}}_{\text{tr}}^{[k]\top} \hat{\mathbf{U}}_{\text{tr}}^{[k]} + 2\mu \mathbf{I})^{-1}$ 
10   $\hat{\mathbf{V}}_{\text{tr}}^{[k]} \leftarrow (\mathbf{Y}_{\text{tr}}^\top \hat{\mathbf{U}}_{\text{tr}}^{[k]} + \Phi_{\text{tr}}^\top \hat{\mathbf{U}}_{\text{te}}^{[k]}) \mathbf{C}_4$ 
11   $\hat{\mathbf{V}}_{\text{te}}^{[k]} \leftarrow \Phi_{\text{te}}^\top \hat{\mathbf{U}}_{\text{te}}^{[k]} (\hat{\mathbf{U}}_{\text{te}}^{[k]\top} \hat{\mathbf{U}}_{\text{te}}^{[k]} + 2\mu \mathbf{I})^{-1}$ 
12   $k \leftarrow k + 1$ 
13 end
14  $\hat{\mathbf{Y}}_{\text{tr}} \leftarrow \hat{\mathbf{U}}_{\text{tr}}^{[k]} \hat{\mathbf{V}}_{\text{tr}}^{[k]\top}$  and  $\hat{\mathbf{Y}}_{\text{te}} \leftarrow \hat{\mathbf{U}}_{\text{tr}}^{[k]} \hat{\mathbf{V}}_{\text{te}}^{[k]\top}$ 

```

Algorithm 2: Threshold Learning

Data: Predicted output matrices $\hat{\mathbf{Y}}_{\text{tr}}$ and $\hat{\mathbf{Y}}_{\text{te}}$, true training output \mathbf{Y}_{tr}
Result: Set of thresholds, one per row $\{\tau_j\}_{j \geq 1}$

```

1 for each row  $j$  of  $\hat{\mathbf{Y}}_{\text{tr}}$  do
2   Store row  $j$  of  $\hat{\mathbf{Y}}_{\text{tr}}$  in a separate vector  $\mathbf{y} \leftarrow \hat{\mathbf{Y}}_{j,\text{tr}}$ 
3   Sort  $\mathbf{y}$  in ascending order  $\mathbf{y} \leftarrow \text{sort}(\mathbf{y})$ 
4    $c_j \leftarrow \|\mathbf{y}\|_0$  // number of non-zero elements in  $\mathbf{y}$ 
5   for  $i \geq c_j$  do
6      $\tau_{j,i} \leftarrow y_i$ 
7      $\hat{\mathbf{Y}}_{j,m,\text{tr}} \leftarrow \mathbb{1}\{\hat{\mathbf{Y}}_{j,m,\text{tr}} \geq \tau_{j,i}\}$  for all  $m \geq 1$ 
8     Calculate the error  $e_{j,i} \leftarrow \|\hat{\mathbf{Y}}_{\text{tr}} - \mathbf{Y}_{\text{tr}}\|_0$ 
9   end
10  Set  $\tau_j \leftarrow \tau_{j,i^*}$ , where  $i^* \leftarrow \arg \min_{i \geq c_j} e_{j,i}$ 
11 end

```

3.2 Sublinear Convergence to a Block Coordinate-Wise Minimizer

In this section, we demonstrate that the block coordinate descent algorithm above converges to a coordinate-wise minimizer (a Nash point). The convergence follows from the strong convexity of the objective functions of the sub-problems as we demonstrate in Lemma 1 below. We will also prove that the convergence rate is sub-linear, and we will

require estimates for the Lipschitz bounds on the gradients of our objective functions. Hence, before stating our results formally and proving them, we will next demonstrate that the sub-problems have strongly convex objective functions and provide Lipschitz bounds on their gradients.

Strong Convexity: A function $f : \mathbb{R}^{p \times q} \rightarrow \mathbb{R}$ is λ -strongly convex, for some $\lambda > 0$, if for all $\mathbf{G}_1, \mathbf{G}_2 \in \mathbb{R}^{p \times q}$

$$f(\mathbf{G}_1) - f(\mathbf{G}_2) \geq \langle \partial_{\mathbf{G}} f(\mathbf{G}_2), \mathbf{G}_1 - \mathbf{G}_2 \rangle + \frac{\lambda}{2} \|\mathbf{G}_1 - \mathbf{G}_2\|_{\text{F}}^2 \quad (44)$$

or, equivalently,

$$\langle \partial_{\mathbf{G}} f(\mathbf{G}_1) - \partial_{\mathbf{G}} f(\mathbf{G}_2), \mathbf{G}_1 - \mathbf{G}_2 \rangle \geq \lambda \|\mathbf{G}_1 - \mathbf{G}_2\|_{\text{F}}^2. \quad (45)$$

We will use definition (45) to demonstrate the strong convexity of $F_1^{[k]}, F_2^{[k]}, F_3^{[k]}$, and $F_4^{[k]}$, defined above, for any $k \geq 1$. We begin with $F_1^{[k]}$: for any $\mathbf{U}_1, \mathbf{U}_2 \in \mathbb{R}^{n \times r}$, we have that

$$\begin{aligned} & \langle \partial_{\mathbf{U}} F_1^{[k]}(\mathbf{U}_1) - \partial_{\mathbf{U}} F_1^{[k]}(\mathbf{U}_2), \mathbf{U}_1 - \mathbf{U}_2 \rangle \\ &= \langle 2(\mathbf{U}_1 - \mathbf{U}_2)(\widehat{\mathbf{V}}_{\text{tr}}^{[k-1]\top} \widehat{\mathbf{V}}_{\text{tr}}^{[k-1]} + \mu \mathbf{I}), \mathbf{U}_1 - \mathbf{U}_2 \rangle \\ &= \text{trace}(2(\widehat{\mathbf{V}}_{\text{tr}}^{[k-1]\top} \widehat{\mathbf{V}}_{\text{tr}}^{[k-1]} + \mu \mathbf{I}) \\ &\quad \times (\mathbf{U}_1 - \mathbf{U}_2)^\top (\mathbf{U}_1 - \mathbf{U}_2)). \end{aligned} \quad (46)$$

Since $\mu > 0$, we have that $2\widehat{\mathbf{V}}_{\text{tr}}^{[k-1]\top} \widehat{\mathbf{V}}_{\text{tr}}^{[k-1]} + 2\mu \mathbf{I}$ is positive definite with positive eigenvalues. In particular the smallest eigenvalue, defined as

$$\underline{\lambda}_1^{[k]} \equiv \min_{1 \leq i \leq r} \lambda(2\widehat{\mathbf{V}}_{\text{tr}}^{[k-1]\top} \widehat{\mathbf{V}}_{\text{tr}}^{[k-1]} + 2\mu \mathbf{I}) \quad (47)$$

is positive, i.e., $\underline{\lambda}_1^{[k]} > 0$, where $\lambda(\mathbf{M})$ is a vector of eigenvalues of \mathbf{M} . It follows immediately that (see, e.g., [7])

$$\begin{aligned} & \langle \partial_{\mathbf{U}} F_1^{[k]}(\mathbf{U}_1) - \partial_{\mathbf{U}} F_1^{[k]}(\mathbf{U}_2), \mathbf{U}_1 - \mathbf{U}_2 \rangle \\ & \geq \underline{\lambda}_1^{[k]} \|\mathbf{U}_1 - \mathbf{U}_2\|_{\text{F}}^2. \end{aligned} \quad (48)$$

Hence, $F_1^{[k]}$ is $\underline{\lambda}_1^{[k]}$ -strongly convex. Similarly,

$$\begin{aligned} & \langle \partial_{\mathbf{U}} F_2^{[k]}(\mathbf{U}_1) - \partial_{\mathbf{U}} F_2^{[k]}(\mathbf{U}_2), \mathbf{U}_1 - \mathbf{U}_2 \rangle \\ & \geq \underline{\lambda}_2^{[k]} \|\mathbf{U}_1 - \mathbf{U}_2\|_{\text{F}}^2 \end{aligned} \quad (49)$$

for any $\mathbf{U}_1, \mathbf{U}_2 \in \mathbb{R}^{h \times r}$, where

$$\begin{aligned} & \underline{\lambda}_2^{[k]} \\ & \equiv \min_{1 \leq i \leq r} \lambda(2\widehat{\mathbf{V}}_{\text{tr}}^{[k-1]\top} \widehat{\mathbf{V}}_{\text{tr}}^{[k-1]} + 2\widehat{\mathbf{V}}_{\text{te}}^{[k-1]\top} \widehat{\mathbf{V}}_{\text{te}}^{[k-1]} + 2\mu \mathbf{I}) \end{aligned} \quad (50)$$

is the smallest eigenvalue of the matrix $2\widehat{\mathbf{V}}_{\text{tr}}^{[k-1]\top} \widehat{\mathbf{V}}_{\text{tr}}^{[k-1]} + 2\widehat{\mathbf{V}}_{\text{te}}^{[k-1]\top} \widehat{\mathbf{V}}_{\text{te}}^{[k-1]} + 2\mu \mathbf{I}$ and $\underline{\lambda}_2^{[k]} > 0$. Hence, $F_2^{[k]}$ is $\underline{\lambda}_2^{[k]}$ -strongly convex. It can be similarly shown that $F_3^{[k]}$ and $F_4^{[k]}$ are $\underline{\lambda}_3^{[k]}$ -strongly convex and $\underline{\lambda}_4^{[k]}$ -strongly convex, respectively, where

$$\underline{\lambda}_3^{[k]} \equiv \min_{1 \leq i \leq r} \lambda(2\widehat{\mathbf{U}}_{\text{tr}}^{[k]\top} \widehat{\mathbf{U}}_{\text{tr}}^{[k]} + 2\widehat{\mathbf{U}}_{\text{te}}^{[k]\top} \widehat{\mathbf{U}}_{\text{te}}^{[k]} + 2\mu \mathbf{I}) \quad (51)$$

and

$$\underline{\lambda}_4^{[k]} \equiv \min_{1 \leq i \leq r} \lambda(2\widehat{\mathbf{U}}_{\text{te}}^{[k]\top} \widehat{\mathbf{U}}_{\text{te}}^{[k]} + 2\mu \mathbf{I}). \quad (52)$$

Lipschitz Bounds: We will now establish that the Lipschitz constants for $\partial_{\mathbf{U}} F_1^{[k]}, \partial_{\mathbf{U}} F_2^{[k]}, \partial_{\mathbf{V}} F_3^{[k]}$, and $\partial_{\mathbf{V}} F_4^{[k]}$ are the largest eigenvalues of the matrices above. For any $\mathbf{U}_1, \mathbf{U}_2 \in \mathbb{R}^{n \times r}$

$$\begin{aligned} & \|\partial_{\mathbf{U}} F_1^{[k]}(\mathbf{U}_1) - \partial_{\mathbf{U}} F_1^{[k]}(\mathbf{U}_2)\|_{\text{F}}^2 \\ &= \|2(\mathbf{U}_1 - \mathbf{U}_2)(\widehat{\mathbf{V}}_{\text{tr}}^{[k-1]\top} \widehat{\mathbf{V}}_{\text{tr}}^{[k-1]} + \mu \mathbf{I})\|_{\text{F}}^2 \\ &\leq (\bar{\lambda}_1^{[k]})^2 \|\mathbf{U}_1 - \mathbf{U}_2\|_{\text{F}}^2, \end{aligned} \quad (53)$$

where

$$\bar{\lambda}_1^{[k]} \equiv \max_{1 \leq i \leq r} \lambda(2\widehat{\mathbf{V}}_{\text{tr}}^{[k-1]\top} \widehat{\mathbf{V}}_{\text{tr}}^{[k-1]} + 2\mu \mathbf{I}). \quad (54)$$

The inequality (53) follows from the bounds in [7] and we have the Lipschitz condition:

$$\|\partial_{\mathbf{U}} F_1^{[k]}(\mathbf{U}_1) - \partial_{\mathbf{U}} F_1^{[k]}(\mathbf{U}_2)\|_{\text{F}}^2 \leq (\bar{\lambda}_1^{[k]})^2 \|\mathbf{U}_1 - \mathbf{U}_2\|_{\text{F}}^2. \quad (55)$$

We can similarly establish the Lipschitz conditions

$$\|\partial_{\mathbf{U}} F_2^{[k]}(\mathbf{U}_1) - \partial_{\mathbf{U}} F_2^{[k]}(\mathbf{U}_2)\|_{\text{F}}^2 \leq (\bar{\lambda}_2^{[k]})^2 \|\mathbf{U}_1 - \mathbf{U}_2\|_{\text{F}}^2, \quad (56)$$

$$\|\partial_{\mathbf{V}} F_3^{[k]}(\mathbf{V}_1) - \partial_{\mathbf{V}} F_3^{[k]}(\mathbf{V}_2)\|_{\text{F}}^2 \leq (\bar{\lambda}_3^{[k]})^2 \|\mathbf{V}_1 - \mathbf{V}_2\|_{\text{F}}^2, \quad (57)$$

and

$$\|\partial_{\mathbf{V}} F_4^{[k]}(\mathbf{V}_1) - \partial_{\mathbf{V}} F_4^{[k]}(\mathbf{V}_2)\|_{\mathbb{F}}^2 \leq (\bar{\lambda}_4^{[k]})^2 \|\mathbf{V}_1 - \mathbf{V}_2\|_{\mathbb{F}}^2, \quad (58)$$

where the constants are given by

$$\begin{aligned} & \bar{\lambda}_2^{[k]} \\ & \equiv \max_{1 \leq i \leq r} \lambda(2\hat{\mathbf{V}}_{\text{tr}}^{[k-1]\top} \hat{\mathbf{V}}_{\text{tr}}^{[k-1]} + 2\hat{\mathbf{V}}_{\text{te}}^{[k-1]\top} \hat{\mathbf{V}}_{\text{te}}^{[k-1]} + 2\mu\mathbf{I}), \end{aligned} \quad (59)$$

$$\bar{\lambda}_3^{[k]} \equiv \max_{1 \leq i \leq r} \lambda(2\hat{\mathbf{U}}_{\text{tr}}^{[k]\top} \hat{\mathbf{U}}_{\text{tr}}^{[k]} + 2\hat{\mathbf{U}}_{\text{te}}^{[k]\top} \hat{\mathbf{U}}_{\text{te}}^{[k]} + 2\mu\mathbf{I}) \quad (60)$$

and

$$\bar{\lambda}_4^{[k]} \equiv \max_{1 \leq i \leq r} \lambda(2\hat{\mathbf{U}}_{\text{te}}^{[k]\top} \hat{\mathbf{U}}_{\text{te}}^{[k]} + 2\mu\mathbf{I}). \quad (61)$$

The smallest eigenvalues, $\{\bar{\lambda}_i^{[k]}\}_{i=1}^4$ are all bounded from below by 2μ for all k , which we need in the sequel. We can also produce estimates of the largest eigenvalues, $\{\bar{\lambda}_i^{[k]}\}_{i=1}^4$, by appeal to the Perron-Frobenius theorem. We denote these upper bounds by $L_1 \geq \bar{\lambda}_1^{[k]}$, $L_2 \geq \bar{\lambda}_2^{[k]}$, $L_3 \geq \bar{\lambda}_3^{[k]}$, and $L_4 \geq \bar{\lambda}_4^{[k]}$ (for all k) and define the upper bound $L_{\max} \equiv \max\{L_1^2, L_2^2, L_3^2, L_4^2\}$.

Lemma 1 (Algorithm Convergence). *Let F , $F_1^{[k]}$, $F_2^{[k]}$, $F_3^{[k]}$, and $F_4^{[k]}$ be as defined in (29) and (34)–(37), and let the block updates $\hat{\mathbf{U}}_{\text{tr}}^{[k]}$, $\hat{\mathbf{U}}_{\text{te}}^{[k]}$, $\hat{\mathbf{V}}_{\text{tr}}^{[k]}$, and $\hat{\mathbf{V}}_{\text{te}}^{[k]}$ be as given in (38)–(41). Assume that the initial solution $\{\hat{\mathbf{U}}_{\text{tr}}^{[0]}, \hat{\mathbf{U}}_{\text{te}}^{[0]}, \hat{\mathbf{V}}_{\text{tr}}^{[0]}, \hat{\mathbf{V}}_{\text{te}}^{[0]}\}$ is such that $F(\hat{\mathbf{U}}_{\text{tr}}^{[0]}, \hat{\mathbf{U}}_{\text{te}}^{[0]}, \hat{\mathbf{V}}_{\text{tr}}^{[0]}, \hat{\mathbf{V}}_{\text{te}}^{[0]}) < \infty$. Then*

$$\begin{aligned} & \lim_{K \rightarrow \infty} \sum_{k=1}^K \left(\|\hat{\mathbf{U}}_{\text{tr}}^{[k-1]} - \hat{\mathbf{U}}_{\text{tr}}^{[k]}\|_{\mathbb{F}}^2 + \|\hat{\mathbf{U}}_{\text{te}}^{[k-1]} - \hat{\mathbf{U}}_{\text{te}}^{[k]}\|_{\mathbb{F}}^2 \right. \\ & \left. + \|\hat{\mathbf{V}}_{\text{tr}}^{[k-1]} - \hat{\mathbf{V}}_{\text{tr}}^{[k]}\|_{\mathbb{F}}^2 + \|\hat{\mathbf{V}}_{\text{te}}^{[k-1]} - \hat{\mathbf{V}}_{\text{te}}^{[k]}\|_{\mathbb{F}}^2 \right) < \infty. \end{aligned} \quad (62)$$

Proof. Noting that $\hat{\mathbf{U}}_{\text{tr}}^{[k]}$ and $\hat{\mathbf{U}}_{\text{te}}^{[k]}$ minimize $F_1^{[k]}$ and $F_2^{[k]}$, respectively, we readily have that

$$\begin{aligned} & 2F(\hat{\mathbf{U}}_{\text{tr}}^{[k-1]}, \hat{\mathbf{U}}_{\text{te}}^{[k-1]}, \hat{\mathbf{V}}_{\text{tr}}^{[k-1]}, \hat{\mathbf{V}}_{\text{te}}^{[k-1]}) - F_1^{[k]}(\hat{\mathbf{U}}_{\text{tr}}^{[k-1]}) \\ & - F_2^{[k]}(\hat{\mathbf{U}}_{\text{te}}^{[k-1]}) - F_3^{[k]}(\hat{\mathbf{V}}_{\text{tr}}^{[k-1]}) - F_4^{[k]}(\hat{\mathbf{V}}_{\text{te}}^{[k-1]}) \geq 0. \end{aligned} \quad (63)$$

Similarly, since $\hat{\mathbf{V}}_{\text{tr}}^{[k]}$ and $\hat{\mathbf{V}}_{\text{te}}^{[k]}$ minimize $F_3^{[k]}$ and $F_4^{[k]}$, respectively, we have that

$$\begin{aligned} & 2F(\hat{\mathbf{U}}_{\text{tr}}^{[k]}, \hat{\mathbf{U}}_{\text{te}}^{[k]}, \hat{\mathbf{V}}_{\text{tr}}^{[k]}, \hat{\mathbf{V}}_{\text{te}}^{[k]}) - F_1^{[k]}(\hat{\mathbf{U}}_{\text{tr}}^{[k]}) \\ & - F_2^{[k]}(\hat{\mathbf{U}}_{\text{te}}^{[k]}) - F_3^{[k]}(\hat{\mathbf{V}}_{\text{tr}}^{[k]}) - F_4^{[k]}(\hat{\mathbf{V}}_{\text{te}}^{[k]}) \leq 0. \end{aligned} \quad (64)$$

Then, for all $k \geq 1$

$$\begin{aligned} & F(\hat{\mathbf{U}}_{\text{tr}}^{[k-1]}, \hat{\mathbf{U}}_{\text{te}}^{[k-1]}, \hat{\mathbf{V}}_{\text{tr}}^{[k-1]}, \hat{\mathbf{V}}_{\text{te}}^{[k-1]}) \\ & - F(\hat{\mathbf{U}}_{\text{tr}}^{[k]}, \hat{\mathbf{U}}_{\text{te}}^{[k]}, \hat{\mathbf{V}}_{\text{tr}}^{[k]}, \hat{\mathbf{V}}_{\text{te}}^{[k]}) \geq \frac{1}{2} \left(F_1^{[k]}(\hat{\mathbf{U}}_{\text{tr}}^{[k-1]}) - F_1^{[k]}(\hat{\mathbf{U}}_{\text{tr}}^{[k]}) \right. \\ & + F_2^{[k]}(\hat{\mathbf{U}}_{\text{te}}^{[k-1]}) - F_2^{[k]}(\hat{\mathbf{U}}_{\text{te}}^{[k]}) + F_3^{[k]}(\hat{\mathbf{V}}_{\text{tr}}^{[k-1]}) - F_3^{[k]}(\hat{\mathbf{V}}_{\text{tr}}^{[k]}) \\ & \left. + F_4^{[k]}(\hat{\mathbf{V}}_{\text{te}}^{[k-1]}) - F_4^{[k]}(\hat{\mathbf{V}}_{\text{te}}^{[k]}) \right). \end{aligned} \quad (65)$$

Since $F_1^{[k]}$ is strongly convex, we have that

$$\begin{aligned} & \frac{1}{2} (F_1^{[k]}(\hat{\mathbf{U}}_{\text{tr}}^{[k-1]}) - F_1^{[k]}(\hat{\mathbf{U}}_{\text{tr}}^{[k]})) \\ & \geq \frac{1}{2} \langle \partial_{\mathbf{U}} F_1^{[k]}(\hat{\mathbf{U}}_{\text{tr}}^{[k]}), \hat{\mathbf{U}}_{\text{tr}}^{[k-1]} - \hat{\mathbf{U}}_{\text{tr}}^{[k]} \rangle \\ & \quad + \frac{\lambda_1^{[k]}}{4} \|\hat{\mathbf{U}}_{\text{tr}}^{[k-1]} - \hat{\mathbf{U}}_{\text{tr}}^{[k]}\|_{\mathbb{F}}^2. \end{aligned} \quad (66)$$

Since $\partial_{\mathbf{U}} F_1^{[k]}(\hat{\mathbf{U}}_{\text{tr}}^{[k]}) = \mathbf{0}$ and $\lambda_1^{[k]} \geq 2\mu$ in accord with the definition (47), we have that

$$\frac{1}{2} (F_1^{[k]}(\hat{\mathbf{U}}_{\text{tr}}^{[k-1]}) - F_1^{[k]}(\hat{\mathbf{U}}_{\text{tr}}^{[k]})) \geq \frac{\mu}{2} \|\hat{\mathbf{U}}_{\text{tr}}^{[k-1]} - \hat{\mathbf{U}}_{\text{tr}}^{[k]}\|_{\mathbb{F}}^2. \quad (67)$$

Similarly, we have that

$$\frac{1}{2} (F_2^{[k]}(\hat{\mathbf{U}}_{\text{te}}^{[k-1]}) - F_2^{[k]}(\hat{\mathbf{U}}_{\text{te}}^{[k]})) \geq \frac{\mu}{2} \|\hat{\mathbf{U}}_{\text{te}}^{[k-1]} - \hat{\mathbf{U}}_{\text{te}}^{[k]}\|_{\mathbb{F}}^2, \quad (68)$$

$$\frac{1}{2} (F_3^{[k]}(\hat{\mathbf{V}}_{\text{tr}}^{[k-1]}) - F_3^{[k]}(\hat{\mathbf{V}}_{\text{tr}}^{[k]})) \geq \frac{\mu}{2} \|\hat{\mathbf{V}}_{\text{tr}}^{[k-1]} - \hat{\mathbf{V}}_{\text{tr}}^{[k]}\|_{\mathbb{F}}^2, \quad (69)$$

and

$$\frac{1}{2} (F_4^{[k]}(\hat{\mathbf{V}}_{\text{te}}^{[k-1]}) - F_4^{[k]}(\hat{\mathbf{V}}_{\text{te}}^{[k]})) \geq \frac{\mu}{2} \|\hat{\mathbf{V}}_{\text{te}}^{[k-1]} - \hat{\mathbf{V}}_{\text{te}}^{[k]}\|_{\mathbb{F}}^2. \quad (70)$$

Combining (65) with (67)–(70) and summing over k from $k = 1$ to $k = K$, we have that

$$\begin{aligned} & \frac{2}{\mu} \left(F(\hat{\mathbf{U}}_{\text{tr}}^{[0]}, \hat{\mathbf{U}}_{\text{te}}^{[0]}, \hat{\mathbf{V}}_{\text{tr}}^{[0]}, \hat{\mathbf{V}}_{\text{te}}^{[0]}) - F(\hat{\mathbf{U}}_{\text{tr}}^{[K]}, \hat{\mathbf{U}}_{\text{te}}^{[K]}, \hat{\mathbf{V}}_{\text{tr}}^{[K]}, \hat{\mathbf{V}}_{\text{te}}^{[K]}) \right) \\ & \geq \sum_{k=1}^K \left(\|\hat{\mathbf{U}}_{\text{tr}}^{[k-1]} - \hat{\mathbf{U}}_{\text{tr}}^{[k]}\|_{\mathbb{F}}^2 + \|\hat{\mathbf{U}}_{\text{te}}^{[k-1]} - \hat{\mathbf{U}}_{\text{te}}^{[k]}\|_{\mathbb{F}}^2 \right. \\ & \quad \left. + \|\hat{\mathbf{V}}_{\text{tr}}^{[k-1]} - \hat{\mathbf{V}}_{\text{tr}}^{[k]}\|_{\mathbb{F}}^2 + \|\hat{\mathbf{V}}_{\text{te}}^{[k-1]} - \hat{\mathbf{V}}_{\text{te}}^{[k]}\|_{\mathbb{F}}^2 \right). \end{aligned} \quad (71)$$

Noting that $F(\mathbf{U}_{\text{tr}}, \mathbf{U}_{\text{te}}, \mathbf{V}_{\text{tr}}, \mathbf{V}_{\text{te}}) \geq 0$ for any $\{\mathbf{U}_{\text{tr}}, \mathbf{U}_{\text{te}}, \mathbf{V}_{\text{tr}}, \mathbf{V}_{\text{te}}\}$ and taking $K \rightarrow \infty$ completes the proof. \square

Corollary 1. *The sequence $\{F(\hat{\mathbf{U}}_{\text{tr}}^{[k]}, \hat{\mathbf{U}}_{\text{te}}^{[k]}, \hat{\mathbf{V}}_{\text{tr}}^{[k]}, \hat{\mathbf{V}}_{\text{te}}^{[k]})\}_{k \geq 0}$ is non-increasing. Moreover, there exists a constant $0 < C_0 \leq \frac{2}{\mu} F(\hat{\mathbf{U}}_{\text{tr}}^{[0]}, \hat{\mathbf{U}}_{\text{te}}^{[0]}, \hat{\mathbf{V}}_{\text{tr}}^{[0]}, \hat{\mathbf{V}}_{\text{te}}^{[0]})$ such that*

$$C_0 \geq \|\hat{\mathbf{U}}_{\text{tr}}^{[k-1]} - \hat{\mathbf{U}}_{\text{tr}}^{[k]}\|_F^2 + \|\hat{\mathbf{U}}_{\text{te}}^{[k-1]} - \hat{\mathbf{U}}_{\text{te}}^{[k]}\|_F^2 + \|\hat{\mathbf{V}}_{\text{tr}}^{[k-1]} - \hat{\mathbf{V}}_{\text{tr}}^{[k]}\|_F^2 + \|\hat{\mathbf{V}}_{\text{te}}^{[k-1]} - \hat{\mathbf{V}}_{\text{te}}^{[k]}\|_F^2 \quad (72)$$

for any $k \geq 1$.

Proof. The first assertion follows immediately from (65) and (67) - (70). The second assertion follows immediately from the first assertion and (71). \square

Lemma 1 implies convergence (in the ℓ_2 sense) to a limit point, that is, (62) implies that as $k \rightarrow \infty$, $\|\hat{\mathbf{U}}_{\text{te}}^{[k-1]} - \hat{\mathbf{U}}_{\text{te}}^{[k]}\|_F^2 \rightarrow 0$, $\|\hat{\mathbf{U}}_{\text{tr}}^{[k-1]} - \hat{\mathbf{U}}_{\text{tr}}^{[k]}\|_F^2 \rightarrow 0$, $\|\hat{\mathbf{V}}_{\text{tr}}^{[k-1]} - \hat{\mathbf{V}}_{\text{tr}}^{[k]}\|_F^2 \rightarrow 0$, $\|\hat{\mathbf{V}}_{\text{te}}^{[k-1]} - \hat{\mathbf{V}}_{\text{te}}^{[k]}\|_F^2 \rightarrow 0$, and that there exists a solution $\{\bar{\mathbf{U}}_{\text{tr}}, \bar{\mathbf{U}}_{\text{te}}, \bar{\mathbf{V}}_{\text{tr}}, \bar{\mathbf{V}}_{\text{te}}\}$, such that

$$\|\hat{\mathbf{U}}_{\text{tr}}^{[k]} - \bar{\mathbf{U}}_{\text{tr}}\|_F^2 + \|\hat{\mathbf{U}}_{\text{te}}^{[k]} - \bar{\mathbf{U}}_{\text{te}}\|_F^2 + \|\hat{\mathbf{V}}_{\text{tr}}^{[k]} - \bar{\mathbf{V}}_{\text{tr}}\|_F^2 + \|\hat{\mathbf{V}}_{\text{te}}^{[k]} - \bar{\mathbf{V}}_{\text{te}}\|_F^2 \xrightarrow[k \rightarrow \infty]{} 0. \quad (73)$$

We prove that the convergence rate is sub-linear. To do so, we next state a well-known result (see for example [1, Lemma 3.5]), which we provide for the sake of completeness.

Lemma 2. *Let $\{q_k\}_{k \geq 0}$ be a non-increasing sequence of positive real numbers and let $0 < \bar{q} < \infty$ and $0 < C < \infty$ be two positive constants. Define $B \equiv \frac{C}{\bar{q}}$ and assume that (i) $q_0 < \bar{q}$ and (ii) $q_{k-1} - q_k \geq C^{-1}q_{k-1}^2$. Then*

$$q_k \leq \frac{C}{B + k}. \quad (74)$$

Proof. The second condition implies that

$$\frac{1}{q_k} - \frac{1}{q_{k-1}} = \frac{q_{k-1} - q_k}{q_{k-1}q_k} \geq \frac{q_{k-1}^2}{C(q_{k-1}q_k)} = \frac{1}{C} \frac{q_{k-1}}{q_k} \geq \frac{1}{C}. \quad (75)$$

Then

$$\frac{1}{q_k} \geq \frac{1}{q_0} + \frac{k}{C} \geq \bar{q}^{-1} + \frac{k}{C}, \quad (76)$$

which completes the proof. \square

Lemma 3. *Assume the conditions of Lemma 1 hold. Assume that $\partial_{\mathbf{U}} F_1^{[k]}(\hat{\mathbf{U}}_{\text{tr}}^{[k-1]}) \neq \mathbf{0}$, $\partial_{\mathbf{U}} F_2^{[k]}(\hat{\mathbf{U}}_{\text{te}}^{[k-1]}) \neq \mathbf{0}$, $\partial_{\mathbf{V}} F_3^{[k]}(\hat{\mathbf{V}}_{\text{tr}}^{[k-1]}) \neq \mathbf{0}$, and $\partial_{\mathbf{V}} F_4^{[k]}(\hat{\mathbf{V}}_{\text{te}}^{[k-1]}) \neq \mathbf{0}$. Let*

$$\Sigma^{[k]} \equiv \tilde{C} \left(F_1^{[k]}(\hat{\mathbf{U}}_{\text{tr}}^{[k]}) + F_2^{[k]}(\hat{\mathbf{U}}_{\text{te}}^{[k]}) + F_3^{[k]}(\hat{\mathbf{V}}_{\text{tr}}^{[k]}) + F_4^{[k]}(\hat{\mathbf{V}}_{\text{te}}^{[k]}) \right)^2 \quad (77)$$

and

$$\Delta^{[k]} \equiv \|\partial_{\mathbf{U}} F_1^{[k]}(\hat{\mathbf{U}}_{\text{tr}}^{[k-1]})\|_F^2 + \|\partial_{\mathbf{U}} F_2^{[k]}(\hat{\mathbf{U}}_{\text{te}}^{[k-1]})\|_F^2 + \|\partial_{\mathbf{V}} F_3^{[k]}(\hat{\mathbf{V}}_{\text{tr}}^{[k-1]})\|_F^2 + \|\partial_{\mathbf{V}} F_4^{[k]}(\hat{\mathbf{V}}_{\text{te}}^{[k-1]})\|_F^2. \quad (78)$$

Then there exists a positive constant $0 < \bar{C}_0 < \infty$, which only depends on the initial solution $(\hat{\mathbf{U}}_{\text{tr}}^{[0]}, \hat{\mathbf{U}}_{\text{te}}^{[0]}, \hat{\mathbf{V}}_{\text{tr}}^{[0]}, \hat{\mathbf{V}}_{\text{te}}^{[0]})$ such that

$$\bar{C}_0 \geq 1 + \frac{\Sigma^{[k]}}{\Delta^{[k]}} \quad (79)$$

for any positive constant $0 < \tilde{C} < \infty$ and all $k \geq 1$.

Proof. Define a constant \tilde{C}_1 so that $\tilde{C}_1 \geq F_1^{[0]}(\hat{\mathbf{U}}_{\text{tr}}^{[0]}) + F_2^{[0]}(\hat{\mathbf{U}}_{\text{te}}^{[0]}) + F_3^{[0]}(\hat{\mathbf{V}}_{\text{tr}}^{[0]}) + F_4^{[0]}(\hat{\mathbf{V}}_{\text{te}}^{[0]})$. Then from (63), (64), and Corollary 1, we have that $\tilde{C}_1 \geq F_1^{[k]}(\hat{\mathbf{U}}_{\text{tr}}^{[k]}) + F_2^{[k]}(\hat{\mathbf{U}}_{\text{te}}^{[k]}) + F_3^{[k]}(\hat{\mathbf{V}}_{\text{tr}}^{[k]}) + F_4^{[k]}(\hat{\mathbf{V}}_{\text{te}}^{[k]})$ for all $k \geq 1$. Next, define

$$\mathcal{K} \equiv \{k : \partial_{\mathbf{U}} F_1^{[k]}(\hat{\mathbf{U}}_{\text{tr}}^{[k-1]}) \neq \mathbf{0}, \partial_{\mathbf{U}} F_2^{[k]}(\hat{\mathbf{U}}_{\text{te}}^{[k-1]}) \neq \mathbf{0}, \partial_{\mathbf{V}} F_3^{[k]}(\hat{\mathbf{V}}_{\text{tr}}^{[k-1]}) \neq \mathbf{0}, \partial_{\mathbf{V}} F_4^{[k]}(\hat{\mathbf{V}}_{\text{te}}^{[k-1]}) \neq \mathbf{0}\}. \quad (80)$$

We immediately have that there exists constants $0 < \tilde{C}_2^{[k]} < \infty$ so that

$$\tilde{C}_2^{[k]} \leq \|\partial_{\mathbf{U}} F_1^{[k]}(\hat{\mathbf{U}}_{\text{tr}}^{[k-1]})\|_F^2 + \|\partial_{\mathbf{U}} F_2^{[k]}(\hat{\mathbf{U}}_{\text{te}}^{[k-1]})\|_F^2 + \|\partial_{\mathbf{V}} F_3^{[k]}(\hat{\mathbf{V}}_{\text{tr}}^{[k-1]})\|_F^2 + \|\partial_{\mathbf{V}} F_4^{[k]}(\hat{\mathbf{V}}_{\text{te}}^{[k-1]})\|_F^2 = \Delta^{[k]} \quad (81)$$

for all $k \in \mathcal{K}$. Define the lower bound

$$\tilde{C}_2 \equiv \inf_{k \in \mathcal{K}} \tilde{C}_2^{[k]}; \quad (82)$$

then, for all $k \in \mathcal{K}$,

$$\frac{1}{\tilde{C}_2} \geq \frac{1}{\Delta^{[k]}}. \quad (83)$$

\square Letting $\bar{C}_0 = 1 + \tilde{C}_2^{-1} \tilde{C} \tilde{C}_1^2$ completes the proof. \square

The set \mathcal{K} defined in (80) is the set of iteration indices before convergence is achieved. It follows immediately from Lemma 3 that before the algorithm converges (i.e., for $k \in \mathcal{K}$) there exists a positive constant $0 < \bar{C}_0 < \infty$ such that

$$\bar{C}_0 \Delta^{[k]} \geq \Delta^{[k]} + \Sigma^{[k]}. \quad (84)$$

We next prove our first main result related to the speed of convergence of Algorithm 1. Specifically, we prove that the

Theorem 3.1 (Sub-linear Convergence Rate). *Let $F, F_1^{[k]}, F_2^{[k]}, F_3^{[k]}$, and $F_4^{[k]}$ be as defined in (29) and (34)–(37), and let the block updates $\hat{\mathbf{U}}_{\text{tr}}^{[k]}, \hat{\mathbf{U}}_{\text{te}}^{[k]}, \hat{\mathbf{V}}_{\text{tr}}^{[k]}$, and $\hat{\mathbf{V}}_{\text{te}}^{[k]}$ be as given in (38)–(41). Then, there exists two positive constants $0 < B < \infty$ and $0 < C < \infty$ such that, for any $k \geq 0$,*

$$\left| F(\hat{\mathbf{U}}_{\text{tr}}^{[k]}, \hat{\mathbf{U}}_{\text{te}}^{[k]}, \hat{\mathbf{V}}_{\text{tr}}^{[k]}, \hat{\mathbf{V}}_{\text{te}}^{[k]}) - F(\bar{\mathbf{U}}_{\text{tr}}, \bar{\mathbf{U}}_{\text{te}}, \bar{\mathbf{V}}_{\text{tr}}, \bar{\mathbf{V}}_{\text{te}}) \right| \leq \frac{C}{B+k}. \quad (85)$$

Proof. The case $k = 0$ is trivial so we will focus on $k \geq 1$. From (65), (67) – (70), and the Lipschitz bounds (55) – (56), we have that

$$\begin{aligned} & F(\hat{\mathbf{U}}_{\text{tr}}^{[k-1]}, \hat{\mathbf{U}}_{\text{te}}^{[k-1]}, \hat{\mathbf{V}}_{\text{tr}}^{[k-1]}, \hat{\mathbf{V}}_{\text{te}}^{[k-1]}) \\ & - F(\hat{\mathbf{U}}_{\text{tr}}^{[k]}, \hat{\mathbf{U}}_{\text{te}}^{[k]}, \hat{\mathbf{V}}_{\text{tr}}^{[k]}, \hat{\mathbf{V}}_{\text{te}}^{[k]}) \geq \frac{\mu}{2L_{\max}} \left(\|\partial_{\mathbf{U}} F_1^{[k]}(\hat{\mathbf{U}}_{\text{tr}}^{[k-1]})\|_F^2 \right. \\ & - \|\partial_{\mathbf{U}} F_1^{[k]}(\hat{\mathbf{U}}_{\text{tr}}^{[k]})\|_F^2 + \|\partial_{\mathbf{U}} F_2^{[k]}(\hat{\mathbf{U}}_{\text{te}}^{[k-1]}) - \partial_{\mathbf{U}} F_2^{[k]}(\hat{\mathbf{U}}_{\text{te}}^{[k]})\|_F^2 \\ & + \|\partial_{\mathbf{V}} F_3^{[k]}(\hat{\mathbf{V}}_{\text{tr}}^{[k-1]}) - \partial_{\mathbf{V}} F_3^{[k]}(\hat{\mathbf{V}}_{\text{tr}}^{[k]})\|_F^2 + \|\partial_{\mathbf{V}} F_4^{[k]}(\hat{\mathbf{V}}_{\text{te}}^{[k-1]}) \\ & \left. - \partial_{\mathbf{V}} F_4^{[k]}(\hat{\mathbf{V}}_{\text{te}}^{[k]})\|_F^2 \right) = \frac{\mu}{2L_{\max}} \left(\|\partial_{\mathbf{U}} F_1^{[k]}(\hat{\mathbf{U}}_{\text{tr}}^{[k-1]})\|_F^2 \right. \\ & + \|\partial_{\mathbf{U}} F_2^{[k]}(\hat{\mathbf{U}}_{\text{te}}^{[k-1]})\|_F^2 + \|\partial_{\mathbf{V}} F_3^{[k]}(\hat{\mathbf{V}}_{\text{tr}}^{[k-1]})\|_F^2 \\ & \left. + \|\partial_{\mathbf{V}} F_4^{[k]}(\hat{\mathbf{V}}_{\text{te}}^{[k-1]})\|_F^2 \right). \quad (86) \end{aligned}$$

By convexity of $F_1^{[k]}$ and the Cauchy-Schwartz inequality, we have that

$$\begin{aligned} & F_1^{[k]}(\hat{\mathbf{U}}_{\text{tr}}^{[k-1]}) - F_1^{[k]}(\hat{\mathbf{U}}_{\text{tr}}^{[k]}) \\ & \leq \langle \partial_{\mathbf{U}} F_1^{[k]}(\hat{\mathbf{U}}_{\text{tr}}^{[k-1]}), \hat{\mathbf{U}}_{\text{tr}}^{[k-1]} - \hat{\mathbf{U}}_{\text{tr}}^{[k]} \rangle \\ & \leq \|\partial_{\mathbf{U}} F_1^{[k]}(\hat{\mathbf{U}}_{\text{tr}}^{[k-1]})\|_F \|\hat{\mathbf{U}}_{\text{tr}}^{[k-1]} - \hat{\mathbf{U}}_{\text{tr}}^{[k]}\|_F. \quad (87) \end{aligned}$$

Then

$$\|\partial_{\mathbf{U}} F_1^{[k]}(\hat{\mathbf{U}}_{\text{tr}}^{[k-1]})\|_F^2 \geq \frac{1}{C_0} (F_1^{[k]}(\hat{\mathbf{U}}_{\text{tr}}^{[k-1]}) - F_1^{[k]}(\hat{\mathbf{U}}_{\text{tr}}^{[k]}))^2, \quad (88)$$

where C_0 is the positive constant of Corollary 1. We can write similar bounds for $F_2^{[k]}, F_3^{[k]}$, and $F_4^{[k]}$ to obtain

$$\begin{aligned} & \frac{1}{4C_0} \left(F_1^{[k]}(\hat{\mathbf{U}}_{\text{tr}}^{[k-1]}) + F_2^{[k]}(\hat{\mathbf{U}}_{\text{te}}^{[k-1]}) + F_3^{[k]}(\hat{\mathbf{V}}_{\text{tr}}^{[k-1]}) \right. \\ & + F_4^{[k]}(\hat{\mathbf{V}}_{\text{te}}^{[k-1]}) - F_1^{[k]}(\hat{\mathbf{U}}_{\text{tr}}^{[k]}) - F_2^{[k]}(\hat{\mathbf{U}}_{\text{te}}^{[k]}) - F_3^{[k]}(\hat{\mathbf{V}}_{\text{tr}}^{[k]}) \\ & \left. - F_4^{[k]}(\hat{\mathbf{V}}_{\text{te}}^{[k]}) \right)^2 \leq \|\partial_{\mathbf{U}} F_1^{[k]}(\hat{\mathbf{U}}_{\text{tr}}^{[k-1]})\|_F^2 + \|\partial_{\mathbf{U}} F_2^{[k]}(\hat{\mathbf{U}}_{\text{te}}^{[k-1]})\|_F^2 \\ & + \|\partial_{\mathbf{U}} F_3^{[k]}(\hat{\mathbf{V}}_{\text{tr}}^{[k-1]})\|_F^2 + \|\partial_{\mathbf{U}} F_4^{[k]}(\hat{\mathbf{V}}_{\text{te}}^{[k-1]})\|_F^2, \quad (89) \end{aligned}$$

where the left hand side follows from the triangle inequality. Applying the reverse triangle inequality, we get

$$\begin{aligned} & \frac{1}{4C_0} \left(F_1^{[k]}(\hat{\mathbf{U}}_{\text{tr}}^{[k-1]}) + F_2^{[k]}(\hat{\mathbf{U}}_{\text{te}}^{[k-1]}) + F_3^{[k]}(\hat{\mathbf{V}}_{\text{tr}}^{[k-1]}) \right. \\ & + F_4^{[k]}(\hat{\mathbf{V}}_{\text{te}}^{[k-1]}) \Big)^2 \leq \frac{1}{4C_0} \left(F_1^{[k]}(\hat{\mathbf{U}}_{\text{tr}}^{[k]}) + F_2^{[k]}(\hat{\mathbf{U}}_{\text{te}}^{[k]}) \right. \\ & + F_3^{[k]}(\hat{\mathbf{V}}_{\text{tr}}^{[k]}) + F_4^{[k]}(\hat{\mathbf{V}}_{\text{te}}^{[k]}) \Big)^2 + \|\partial_{\mathbf{U}} F_1^{[k]}(\hat{\mathbf{U}}_{\text{tr}}^{[k-1]})\|_F^2 \\ & + \|\partial_{\mathbf{U}} F_2^{[k]}(\hat{\mathbf{U}}_{\text{te}}^{[k-1]})\|_F^2 + \|\partial_{\mathbf{U}} F_3^{[k]}(\hat{\mathbf{V}}_{\text{tr}}^{[k-1]})\|_F^2 \\ & + \|\partial_{\mathbf{U}} F_4^{[k]}(\hat{\mathbf{V}}_{\text{te}}^{[k-1]})\|_F^2. \quad (90) \end{aligned}$$

It can be easily shown that

$$\begin{aligned} & F(\hat{\mathbf{U}}_{\text{tr}}^{[k-1]}, \hat{\mathbf{U}}_{\text{te}}^{[k-1]}, \hat{\mathbf{V}}_{\text{tr}}^{[k-1]}, \hat{\mathbf{V}}_{\text{te}}^{[k-1]}) \\ & \leq F_1^{[k]}(\hat{\mathbf{U}}_{\text{tr}}^{[k-1]}) + F_2^{[k]}(\hat{\mathbf{U}}_{\text{te}}^{[k-1]}) + F_3^{[k]}(\hat{\mathbf{V}}_{\text{tr}}^{[k-1]}) \\ & + F_4^{[k]}(\hat{\mathbf{V}}_{\text{te}}^{[k-1]}). \quad (91) \end{aligned}$$

Hence,

$$\begin{aligned} & \frac{1}{4C_0} \left(F(\hat{\mathbf{U}}_{\text{tr}}^{[k-1]}, \hat{\mathbf{U}}_{\text{te}}^{[k-1]}, \hat{\mathbf{V}}_{\text{tr}}^{[k-1]}, \hat{\mathbf{V}}_{\text{te}}^{[k-1]}) \right)^2 \\ & \leq \frac{1}{4C_0} \left(F_1^{[k]}(\hat{\mathbf{U}}_{\text{tr}}^{[k]}) + F_2^{[k]}(\hat{\mathbf{U}}_{\text{te}}^{[k]}) + F_3^{[k]}(\hat{\mathbf{V}}_{\text{tr}}^{[k]}) \right. \\ & + F_4^{[k]}(\hat{\mathbf{V}}_{\text{te}}^{[k]}) \Big)^2 + \|\partial_{\mathbf{U}} F_1^{[k]}(\hat{\mathbf{U}}_{\text{tr}}^{[k-1]})\|_F^2 \\ & + \|\partial_{\mathbf{U}} F_2^{[k]}(\hat{\mathbf{U}}_{\text{te}}^{[k-1]})\|_F^2 + \|\partial_{\mathbf{U}} F_3^{[k]}(\hat{\mathbf{V}}_{\text{tr}}^{[k-1]})\|_F^2 \\ & + \|\partial_{\mathbf{U}} F_4^{[k]}(\hat{\mathbf{V}}_{\text{te}}^{[k-1]})\|_F^2. \quad (92) \end{aligned}$$

From (84) (and Lemma 3) we have that there exists a positive constant \bar{C}_0 which only depends on the initial solution so that (92) implies that

$$\begin{aligned} & \frac{1}{4C_0\bar{C}_0} \left(F(\hat{\mathbf{U}}_{\text{tr}}^{[k-1]}, \hat{\mathbf{U}}_{\text{te}}^{[k-1]}, \hat{\mathbf{V}}_{\text{tr}}^{[k-1]}, \hat{\mathbf{V}}_{\text{te}}^{[k-1]}) \right)^2 \\ & \leq \|\partial_{\mathbf{U}} F_1^{[k]}(\hat{\mathbf{U}}_{\text{tr}}^{[k-1]})\|_F^2 + \|\partial_{\mathbf{U}} F_2^{[k]}(\hat{\mathbf{U}}_{\text{te}}^{[k-1]})\|_F^2 \\ & \quad + \|\partial_{\mathbf{U}} F_3^{[k]}(\hat{\mathbf{V}}_{\text{tr}}^{[k-1]})\|_F^2 + \|\partial_{\mathbf{U}} F_4^{[k]}(\hat{\mathbf{V}}_{\text{te}}^{[k-1]})\|_F^2. \end{aligned} \quad (93)$$

Combining this with (86), we get

$$\begin{aligned} & F(\hat{\mathbf{U}}_{\text{tr}}^{[k-1]}, \hat{\mathbf{U}}_{\text{te}}^{[k-1]}, \hat{\mathbf{V}}_{\text{tr}}^{[k-1]}, \hat{\mathbf{V}}_{\text{te}}^{[k-1]}) \\ & \quad - F(\hat{\mathbf{U}}_{\text{tr}}^{[k]}, \hat{\mathbf{U}}_{\text{te}}^{[k]}, \hat{\mathbf{V}}_{\text{tr}}^{[k]}, \hat{\mathbf{V}}_{\text{te}}^{[k]}) \\ & \geq \frac{\mu}{8L_{\max}C_0\bar{C}_0} \left(F(\hat{\mathbf{U}}_{\text{tr}}^{[k-1]}, \hat{\mathbf{U}}_{\text{te}}^{[k-1]}, \hat{\mathbf{V}}_{\text{tr}}^{[k-1]}, \hat{\mathbf{V}}_{\text{te}}^{[k-1]}) \right)^2. \end{aligned} \quad (94)$$

Since $F(\hat{\mathbf{U}}_{\text{tr}}^{[k]}, \hat{\mathbf{U}}_{\text{te}}^{[k]}, \hat{\mathbf{V}}_{\text{tr}}^{[k]}, \hat{\mathbf{V}}_{\text{te}}^{[k]}) \geq F(\bar{\mathbf{U}}_{\text{tr}}, \bar{\mathbf{U}}_{\text{te}}, \bar{\mathbf{V}}_{\text{tr}}, \bar{\mathbf{V}}_{\text{te}})$ for all k , (94) implies that

$$\begin{aligned} & F(\hat{\mathbf{U}}_{\text{tr}}^{[k-1]}, \hat{\mathbf{U}}_{\text{te}}^{[k-1]}, \hat{\mathbf{V}}_{\text{tr}}^{[k-1]}, \hat{\mathbf{V}}_{\text{te}}^{[k-1]}) \\ & \quad - F(\hat{\mathbf{U}}_{\text{tr}}^{[k]}, \hat{\mathbf{U}}_{\text{te}}^{[k]}, \hat{\mathbf{V}}_{\text{tr}}^{[k]}, \hat{\mathbf{V}}_{\text{te}}^{[k]}) \\ & \geq \frac{\mu}{8L_{\max}C_0\bar{C}_0} \left(F(\hat{\mathbf{U}}_{\text{tr}}^{[k-1]}, \hat{\mathbf{U}}_{\text{te}}^{[k-1]}, \hat{\mathbf{V}}_{\text{tr}}^{[k-1]}, \hat{\mathbf{V}}_{\text{te}}^{[k-1]}) \right. \\ & \quad \left. - F(\bar{\mathbf{U}}_{\text{tr}}, \bar{\mathbf{U}}_{\text{te}}, \bar{\mathbf{V}}_{\text{tr}}, \bar{\mathbf{V}}_{\text{te}}) \right)^2. \end{aligned} \quad (95)$$

We next add and subtract $F(\bar{\mathbf{U}}_{\text{tr}}, \bar{\mathbf{U}}_{\text{te}}, \bar{\mathbf{V}}_{\text{tr}}, \bar{\mathbf{V}}_{\text{te}})$ on the left hand side, and we invoke Lemma (2) with

$$q_k \equiv F(\hat{\mathbf{U}}_{\text{tr}}^{[k]}, \hat{\mathbf{U}}_{\text{te}}^{[k]}, \hat{\mathbf{V}}_{\text{tr}}^{[k]}, \hat{\mathbf{V}}_{\text{te}}^{[k]}) - F(\bar{\mathbf{U}}_{\text{tr}}, \bar{\mathbf{U}}_{\text{te}}, \bar{\mathbf{V}}_{\text{tr}}, \bar{\mathbf{V}}_{\text{te}}) \quad (96)$$

and note that $\{q_k\}_{k \geq 0}$ is a non-negative sequence by the first assertion of Corollary 1. Letting $B = 16L_{\max}\bar{C}_0\mu^{-2}$ and $C = 8L_{\max}C_0\bar{C}_0\mu^{-1}$ completes the proof. \square

The result in Theorem 3.1 suggests that one can determine a number of iterations as a stopping criterion for Algorithm 1. More importantly, the theorem says that this number need not be large in order to get close to the limit. The next theorem provides our second main result. It demonstrates that the limiting solution $\{\bar{\mathbf{U}}_{\text{tr}}, \bar{\mathbf{U}}_{\text{te}}, \bar{\mathbf{V}}_{\text{tr}}, \bar{\mathbf{V}}_{\text{te}}\}$ implied by Lemma 1 is a block coordinate-wise minimizer of the matrix completion problem (28).

Theorem 3.2 (Block Corrdinate-Wise Minimizer).

Under the assumptions of Lemma 1, the variational inequalities (30)-(33) hold for all $\mathbf{U}_{\text{tr}} \in \mathbb{R}^{n \times r}$, all $\mathbf{U}_{\text{te}} \in \mathbb{R}^{h \times r}$, all $\mathbf{V}_{\text{tr}} \in \mathbb{R}^{T_{\text{tr}} \times r}$, and all $\mathbf{V}_{\text{te}} \in \mathbb{R}^{T_{\text{te}} \times r}$.

Proof. In the limit, we have that

$$\bar{\mathbf{U}}_{\text{tr}} = \arg \min_{\mathbf{U}_{\text{tr}} \in \mathbb{R}^{n \times r}} \|\mathbf{U}_{\text{tr}} \bar{\mathbf{V}}_{\text{tr}}^\top - \mathbf{Y}_{\text{tr}}\|_F^2 + 2\mu \|\mathbf{U}_{\text{tr}}\|_F^2. \quad (97)$$

Hence, for all $\mathbf{U}_{\text{tr}} \in \mathbb{R}^{n \times r}$

$$F(\mathbf{U}_{\text{tr}}, \bar{\mathbf{U}}_{\text{te}}, \bar{\mathbf{V}}_{\text{tr}}, \bar{\mathbf{V}}_{\text{te}}) \geq F(\bar{\mathbf{U}}_{\text{tr}}, \bar{\mathbf{U}}_{\text{te}}, \bar{\mathbf{V}}_{\text{tr}}, \bar{\mathbf{V}}_{\text{te}}). \quad (98)$$

In particular, consider the matrix $\bar{\mathbf{U}}_{\text{tr}} + h(\mathbf{U}_{\text{tr}} - \bar{\mathbf{U}}_{\text{tr}})$, where h is a scalar and \mathbf{U}_{tr} is any $\mathbb{R}^{n \times r}$ matrix. From (98), we have for each $h > 0$ that

$$\begin{aligned} & \frac{1}{h} \left(F(\bar{\mathbf{U}}_{\text{tr}} + h(\mathbf{U}_{\text{tr}} - \bar{\mathbf{U}}_{\text{tr}}), \bar{\mathbf{U}}_{\text{te}}, \bar{\mathbf{V}}_{\text{tr}}, \bar{\mathbf{V}}_{\text{te}}) \right. \\ & \quad \left. - F(\bar{\mathbf{U}}_{\text{tr}}, \bar{\mathbf{U}}_{\text{te}}, \bar{\mathbf{V}}_{\text{tr}}, \bar{\mathbf{V}}_{\text{te}}) \right) \geq 0 \end{aligned} \quad (99)$$

is true for all $\mathbf{U}_{\text{tr}} \in \mathbb{R}^{n \times r}$. Since F is continuous in all block coordinates, upon taking $h \rightarrow 0$ the left-hand side converges to the directional partial derivative of F along $\mathbf{U}_{\text{tr}} - \bar{\mathbf{U}}_{\text{tr}}$ and since the inequality is true for all h , it is true in the limit. Then, since the directional derivative is simply the inner product of the derivative and the direction, it follows that the first variational inequality,

$$\langle \partial_{\mathbf{U}_{\text{tr}}} F(\bar{\mathbf{U}}_{\text{tr}}, \bar{\mathbf{U}}_{\text{te}}, \bar{\mathbf{V}}_{\text{tr}}, \bar{\mathbf{V}}_{\text{te}}), \mathbf{U}_{\text{tr}} - \bar{\mathbf{U}}_{\text{tr}} \rangle \geq 0, \quad (100)$$

is true for all $\mathbf{U}_{\text{tr}} \in \mathbb{R}^{n \times r}$. The same reasoning can be used to demonstrate that the variational inequalities (31), (32), and (33) also hold for $\bar{\mathbf{U}}_{\text{te}}$, $\bar{\mathbf{V}}_{\text{tr}}$, and $\bar{\mathbf{V}}_{\text{te}}$, respectively. \square

The interpretation of the solution as a Nash point (an equilibrium) can be seen immediately upon examining the inequalities

$$F(\mathbf{U}_{\text{tr}}, \bar{\mathbf{U}}_{\text{te}}, \bar{\mathbf{V}}_{\text{tr}}, \bar{\mathbf{V}}_{\text{te}}) \geq F(\bar{\mathbf{U}}_{\text{tr}}, \bar{\mathbf{U}}_{\text{te}}, \bar{\mathbf{V}}_{\text{tr}}, \bar{\mathbf{V}}_{\text{te}}), \quad (101)$$

$$F(\bar{\mathbf{U}}_{\text{tr}}, \mathbf{U}_{\text{te}}, \bar{\mathbf{V}}_{\text{tr}}, \bar{\mathbf{V}}_{\text{te}}) \geq F(\bar{\mathbf{U}}_{\text{tr}}, \bar{\mathbf{U}}_{\text{te}}, \bar{\mathbf{V}}_{\text{tr}}, \bar{\mathbf{V}}_{\text{te}}), \quad (102)$$

$$F(\bar{\mathbf{U}}_{\text{tr}}, \bar{\mathbf{U}}_{\text{te}}, \mathbf{V}_{\text{tr}}, \bar{\mathbf{V}}_{\text{te}}) \geq F(\bar{\mathbf{U}}_{\text{tr}}, \bar{\mathbf{U}}_{\text{te}}, \bar{\mathbf{V}}_{\text{tr}}, \bar{\mathbf{V}}_{\text{te}}), \quad (103)$$

and

$$F(\bar{\mathbf{U}}_{\text{tr}}, \bar{\mathbf{U}}_{\text{te}}, \bar{\mathbf{V}}_{\text{tr}}, \mathbf{V}_{\text{te}}) \geq F(\bar{\mathbf{U}}_{\text{tr}}, \bar{\mathbf{U}}_{\text{te}}, \bar{\mathbf{V}}_{\text{tr}}, \bar{\mathbf{V}}_{\text{te}}) \quad (104)$$

for all $\mathbf{U}_{\text{tr}} \in \mathbb{R}^{n \times r}$, $\mathbf{U}_{\text{te}} \in \mathbb{R}^{h \times r}$, $\mathbf{V}_{\text{tr}} \in \mathbb{R}^{T_{\text{tr}} \times r}$, and $\mathbf{V}_{\text{te}} \in \mathbb{R}^{T_{\text{te}} \times r}$. The inequalities (102), (103), and (104) can be established in the same way that (101) was established in the proof of Theorem 3.2.

4 Ensemble Learning and Time Complexity

4.1 Incorporating Historical Patterns

We extend the solution approach presented above to capture and incorporate patterns that may exist in the data. The extension leverages the “big-ness” of high-resolution traffic data. To this end, we employ a boosting technique in which the ensembles represent past days. Boosting has become a standard component of online learning algorithms; it has been established that they improve solution quality, both experimentally and analytically [8].

Our proposed ensemble learning implementation considers past ensembles of training datasets as part of the prediction process. Without loss of generality, let \mathcal{D} be set of indices of past ensembles and each ensemble corresponds to a day in the past with lower indices representing more recent days, in particular, $d = 1$ corresponds to the ‘present’. The set \mathcal{D} is typically chosen to include 4-5 weeks of past data and either week days or week ends are chosen based on whether the present day is a week day or week end. Let $\theta(t, d)$ denote that weight associated with time step t in ensemble d . The joint matrix is now given by

$$\mathbf{Z}(\Theta) \equiv \begin{bmatrix} \mathbf{Y}_{|\mathcal{D}|, \text{tr}} & \cdots & \mathbf{Y}_{1, \text{tr}} & \mathbf{Y}_{\text{te}} \\ \Theta_{|\mathcal{D}|} \odot \Phi(\mathbf{X}_{|\mathcal{D}|, \text{tr}}) & \cdots & \Theta_1 \odot \Phi(\mathbf{X}_{1, \text{tr}}) & \Phi_{\text{te}} \end{bmatrix}, \quad (105)$$

where $\mathbf{Y}_{d, \text{tr}} \equiv [\mathbf{y}_{d, \text{tr}}(1) \cdots \mathbf{y}_{d, \text{tr}}(T_{\text{tr}})]$ and $\mathbf{X}_{d, \text{tr}} \equiv [\mathbf{B}_L \mathbf{x}_{d, \text{tr}}(1) \cdots \mathbf{B}_L \mathbf{x}_{d, \text{tr}}(T_{\text{tr}})]$ are the output and input matrices, respectively, corresponding to day d , Φ applies the (unknown) mapping function to each of the columns of its argument,

$$\Theta_d \equiv [\theta(1, d) \mathbf{e} \cdots \theta(T_{\text{tr}}, d) \mathbf{e}] \in \mathbb{R}^{h \times T_{\text{tr}}} \quad (106)$$

is a matrix of weights corresponding to day d , \mathbf{e} is vector of 1s of dimension h , and \odot is the component-wise (or Hadamard) product. Given $\{\theta(t, d)\}_{1 \leq t \leq T_{\text{tr}}, d \in \mathcal{D}}$, the prediction problem is simply a matrix completion problem, which is solved by block coordinate descent. Here, the training data are given by the augmented matrices

$$\tilde{\mathbf{Y}}_{\text{tr}} \equiv [\mathbf{Y}_{|\mathcal{D}|, \text{tr}} \cdots \mathbf{Y}_{1, \text{tr}}] \in \mathbb{R}^{n \times |\mathcal{D}| T_{\text{tr}}} \quad (107)$$

and

$$\tilde{\Phi}_{\text{tr}}(\Theta) \equiv [\Theta_{|\mathcal{D}|} \odot \Phi(\mathbf{X}_{|\mathcal{D}|, \text{tr}}) \cdots \Theta_1 \odot \Phi(\mathbf{X}_{1, \text{tr}})] \in \mathbb{R}^{h \times |\mathcal{D}| T_{\text{tr}}}. \quad (108)$$

The joint matrix is given by

$$\mathbf{Z}(\Theta) \equiv \begin{bmatrix} \tilde{\mathbf{Y}}_{\text{tr}} & \mathbf{Y}_{\text{te}} \\ \tilde{\Phi}_{\text{tr}}(\Theta) & \Phi_{\text{te}} \end{bmatrix} \in \mathbb{R}^{(n+h) \times (|\mathcal{D}| T_{\text{tr}} + T_{\text{te}})}. \quad (109)$$

The overall prediction algorithm is depicted in Fig. 2. The procedure begins with an initial set of

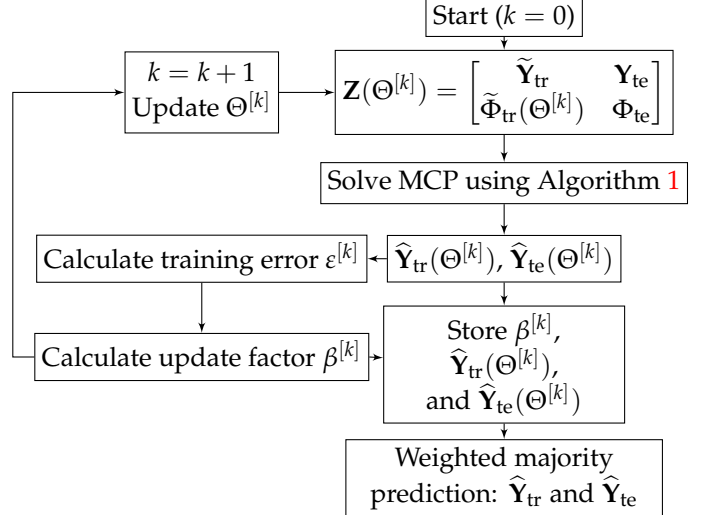


Figure 2: An Illustration of the Overall Prediction Algorithm with Adaptive Boosting.

weights, which can be chosen in a variety of ways, e.g., equal weights: $\theta^{[0]}(t, d) \propto 1$ for all $t \in \{1, \dots, T_{\text{tr}}\}$ and $d \in \mathcal{D}$, or weights that favor more recent days: $\theta^{[0]}(t, d) \propto d^{-1}$. (In our experiments, we use the former.) We then solve the matrix completion problem

using Algorithm 1 and use the results to calculate the training error, which is given as

$$\varepsilon^{[k]} = \frac{\sum_{(t,d)} \theta^{[k]}(t,d) \mathbb{1}\{\hat{\mathbf{y}}_{d,\text{tr}}^{[k]}(t) \neq \mathbf{y}_{d,\text{tr}}(t)\}}{\sum_{(t,d)} \theta^{[k]}(t,d)}, \quad (110)$$

where $\hat{\mathbf{y}}_{d,\text{tr}}^{[k]}(t)$ is the training output produced by Algorithm 1 using the weights determined in iteration k , $\Theta^{[k]}$. This error metric is bounded between 0 and 1, $\varepsilon^{[k]} = 0$ indicates that $\hat{\mathbf{y}}_{d,\text{tr}}^{[k]}(t) = \mathbf{y}_{d,\text{tr}}(t)$ for all (t,d) pairs and, at the other extreme, $\varepsilon^{[k]} = 1$ indicates that $\hat{\mathbf{y}}_{d,\text{tr}}^{[k]}(t) \neq \mathbf{y}_{d,\text{tr}}(t)$ for none of the (t,d) pairs. The error is used to calculate an *update factor* as follows:

$$\beta^{[k]} = \log \frac{1 - \varepsilon^{[k]}}{\varepsilon^{[k]}}, \quad (111)$$

which is used to update the weight as

$$\theta^{[k+1]}(t,d) = \theta^{[k]}(t,d) \exp(\beta^{[k]} \mathbb{1}\{\hat{\mathbf{y}}_{d,\text{tr}}^{[k]}(t) \neq \mathbf{y}_{d,\text{tr}}(t)\}). \quad (112)$$

The logarithm in (111) is used to mitigate potential computational instabilities due to large values. As $\varepsilon^{[k]} \rightarrow 0$, $\beta^{[k]} \rightarrow \infty$. The limit corresponds to the case where $\mathbb{1}\{\hat{\mathbf{y}}_{d,\text{tr}}^{[k]}(t) \neq \mathbf{y}_{d,\text{tr}}(t)\} = 0$ for all (t,d) pairs (i.e., a perfect match) so that the exponential function on the right-hand side of (112) is 1. This means that in the case of a perfect match, the weights do not change. On the other hand, as $\varepsilon^{[k]} \rightarrow 1$, $\beta^{[k]} \rightarrow -\infty$ and $\theta^{[k+1]}(t,d) \rightarrow 0$ in this case.

Finally, the test predictions produced over the K iterations are combined to produce the final prediction. Let $\alpha^{[k]}$ denote the weight assigned to the prediction produced in iteration k and let it be defined as follows:

$$\alpha^{[k]} \equiv \frac{\beta^{[k]}}{\sum_{j=1}^K \beta^{[j]}}. \quad (113)$$

The combined predictions are given by

$$\hat{\mathbf{Y}}_{\text{tr}} = \sum_k \alpha^{[k]} \hat{\mathbf{Y}}_{\text{tr}}(\Theta^{[k]}) \quad (114)$$

and

$$\hat{\mathbf{Y}}_{\text{te}} = \sum_k \alpha^{[k]} \hat{\mathbf{Y}}_{\text{te}}(\Theta^{[k]}). \quad (115)$$

This is followed by a thresholding step to translate the predictions to labels in $\{0,1\}$. The prediction algorithm is summarized in Algorithm 3 below. Theorem 4.1 provides a bound on the training error (expressed as the number of mis-matched columns in

$\hat{\mathbf{Y}}_{\text{tr}}$). The error bound given in the theorem illustrates the fast reduction in error with number of iterations. As long as $\varepsilon^{[k]} < 0.5$, the error drops quickly. The bound we give is a specialization of the well known result in [8, Theorem 6] to our context.

Algorithm 3: Prediction with Ensemble Learning

Data: Joint matrix $\mathbf{Z}(\Theta^{[0]})$ and K (maximum number of iterations)

Result: $\hat{\mathbf{Y}}_{\text{tr}}$ and $\hat{\mathbf{Y}}_{\text{te}}$

1 **Initialize:** $k \leftarrow 0$ and initial weights

$$\Theta^{[0]} \equiv [\Theta_{|\mathcal{D}|}^{[0]} \cdots \Theta_1^{[0]}]$$

2 **while** $k < K$ **do**

3 $\tilde{\Phi}_{\text{tr}}(\Theta^{[k]}) \leftarrow$

$$[\Theta_{|\mathcal{D}|}^{[k]} \odot \Phi(\mathbf{X}_{|\mathcal{D}|,\text{tr}}) \cdots \Theta_1^{[k]} \odot \Phi(\mathbf{X}_{1,\text{tr}})]$$

4 Calculate $\hat{\mathbf{Y}}_{\text{tr}}(\Theta^{[k]})$ and $\hat{\mathbf{Y}}_{\text{te}}(\Theta^{[k]})$ using Algorithm 1

5 Calculate $\varepsilon^{[k]}$ and $\beta^{[k]}$ using (110) and (111), respectively

6 $k \leftarrow k + 1$ and update $\Theta^{[k]}$ using (112)

7 **end**

8 Calculate the weighted majority predictions using (114)-(115) and apply thresholding (Algorithm 2).

Theorem 4.1 (Training Error of Algorithm 3). Assume that $\theta^{[0]}(t,d) = 1$ for all (t,d) -pairs and let $\boldsymbol{\tau} \in \mathbb{R}^n$ denote a vector of thresholds. Let

$$\varepsilon(K) \equiv |\{(t,d) : \hat{\mathbf{y}}_{d,\text{tr}}^{[K]}(t) \neq \mathbf{y}_{d,\text{tr}}(t)\}| \quad (116)$$

denote the training sample error at the end of step K . Then

$$\varepsilon(K) \leq 2^K |\mathcal{D}| T_{\text{tr}} \prod_{k=0}^{K-1} (1 - \varepsilon^{[k]})^{\frac{n - \|\boldsymbol{\tau}\|_1}{n}} (\varepsilon^{[k]})^{\frac{\|\boldsymbol{\tau}\|_1}{n}}. \quad (117)$$

Proof. Let (t,d) be such that $\mathbb{1}\{\hat{\mathbf{y}}_{d,\text{tr}}(t) \neq \mathbf{y}_{d,\text{tr}}(t)\} = 1$. Since $\sum_{k=0}^{K-1} \alpha^{[k]} = 1$ we have that $\mathbf{y}_{d,\text{tr}}(t) = \sum_{k=0}^{K-1} \alpha^{[k]} \mathbf{y}_{d,\text{tr}}(t)$, thus

$$\sum_{k=0}^{K-1} \alpha^{[k]} \|\hat{\mathbf{y}}_{d,\text{tr}}^{[k]}(t) - \mathbf{y}_{d,\text{tr}}(t)\|_1 \geq \|\boldsymbol{\tau}\|_1. \quad (118)$$

Multiplying both sides by $n^{-1} \sum_{j=0}^K \beta^{[j]}$, we get the inequality

$$\sum_{k=0}^K \frac{\beta^{[k]}}{n} \|\hat{\mathbf{y}}_{d,\text{tr}}^{[k]}(t) - \mathbf{y}_{d,\text{tr}}(t)\|_1 \geq \frac{1}{n} \sum_{j=0}^K \beta^{[j]} \|\boldsymbol{\tau}\|_1. \quad (119)$$

Since $\mathbb{1}\{\hat{\mathbf{y}}_{d,\text{tr}}^{[k]}(t) \neq \mathbf{y}_{d,\text{tr}}(t)\} \geq n^{-1} \|\hat{\mathbf{y}}_{d,\text{tr}}^{[k]}(t) - \mathbf{y}_{d,\text{tr}}(t)\|_1$ for all k , we have that

$$\sum_{k=0}^K \beta^{[k]} \mathbb{1}\{\hat{\mathbf{y}}_{d,\text{tr}}^{[k]}(t) \neq \mathbf{y}_{d,\text{tr}}(t)\} \geq \frac{1}{n} \sum_{j=0}^K \beta^{[j]} \|\boldsymbol{\tau}\|_1. \quad (120)$$

Define $\mathcal{M}^{[k]} \equiv \{(t, d) : \hat{\mathbf{y}}_{d,\text{tr}}^{[k]}(t) \neq \mathbf{y}_{d,\text{tr}}(t)\}$. It follows from (120) that

$$\begin{aligned} & \sum_{(t,d)} \theta^{[K+1]}(t, d) \\ & \geq \sum_{(t,d) \in \mathcal{M}^{[K]}} \theta^{[0]}(t, d) \exp\left(\sum_{k=0}^K \beta^{[k]} n^{-1} \|\boldsymbol{\tau}\|_1\right) \\ & = \epsilon(K) \prod_{k=0}^K \exp(\beta^{[k]} n^{-1} \|\boldsymbol{\tau}\|_1), \quad (121) \end{aligned}$$

where $\epsilon(K) = \sum_{(t,d) \in \mathcal{M}^{[K]}} \theta^{[0]}(t, d)$ follows from the initialization assumption. Next, we have that

$$\begin{aligned} & \sum_{(t,d)} \theta^{[K+1]}(t, d) \\ & = \sum_{(t,d)} \theta^{[K]}(t, d) \left(\frac{1 - \epsilon^{[K]}}{\epsilon^{[K]}}\right)^{\mathbb{1}\{\hat{\mathbf{y}}_{d,\text{tr}}^{[K]}(t) \neq \mathbf{y}_{d,\text{tr}}(t)\}} \\ & = \sum_{(t,d)} \theta^{[K]}(t, d) \left(1 - \left(1 - \frac{1 - \epsilon^{[K]}}{\epsilon^{[K]}}\right)\right. \\ & \quad \left. \times \mathbb{1}\{\hat{\mathbf{y}}_{d,\text{tr}}^{[K]}(t) \neq \mathbf{y}_{d,\text{tr}}(t)\}\right) \\ & = \sum_{(t,d)} \theta^{[K]}(t, d) - \sum_{(t,d)} \theta^{[K]}(t, d) \mathbb{1}\{\hat{\mathbf{y}}_{d,\text{tr}}^{[K]}(t) \neq \mathbf{y}_{d,\text{tr}}(t)\} \\ & \quad \times \left(1 - \frac{1 - \epsilon^{[K]}}{\epsilon^{[K]}}\right) \\ & = \sum_{(t,d)} \theta^{[K]}(t, d) - \sum_{(t,d)} \theta^{[K]}(t, d) \epsilon^{[K]} \left(1 - \frac{1 - \epsilon^{[K]}}{\epsilon^{[K]}}\right) \\ & = \sum_{(t,d)} 2\theta^{[K]}(t, d) (1 - \epsilon^{[K]}), \quad (122) \end{aligned}$$

where the second to last equality follows from (110). This implies that

$$\sum_{(t,d)} \theta^{[K+1]}(t, d) = 2^K |\mathcal{D}| T_{\text{tr}} \prod_{k=0}^K (1 - \epsilon^{[k]}). \quad (123)$$

Combining (121) with (123) and utilizing the definition of $\beta^{[k]}$, (111), completes the proof. \square

4.2 Time Complexity Analysis

In each iteration, the block-coordinate descent algorithm (Algorithm 1) solves four least-squared (LS) problems but the solutions are given in closed form. The complexity of calculating $\hat{\mathbf{U}}_{\text{tr}}^{[k]}$, using (38), is $O(r^2 T_{\text{tr}})$ (the complexity of matrix multiplication and inversion of a symmetric positive definite matrix). The complexity of updating $\hat{\mathbf{V}}_{\text{tr}}^{[k]}$, using (40), is $O(\max\{r^3, T_{\text{tr}}^2 r, T_{\text{tr}} T_{\text{te}} r\})$, which is typically equal to $O(T_{\text{tr}}^2 r)$ as $T_{\text{tr}} > T_{\text{te}} > r$ will be the case in most settings. Similarly, updating $\hat{\mathbf{V}}_{\text{te}}^{[k]}$ has a time complexity of $O(\max\{r^3, T_{\text{te}}^2 r, T_{\text{tr}} T_{\text{te}} r\})$, which is typically $O(T_{\text{tr}} T_{\text{te}} r)$. Therefore, the complexity in each iteration of Algorithm 1 is $O(\max\{r^3, T_{\text{tr}}^2 r, T_{\text{te}}^2 r, T_{\text{tr}} T_{\text{te}} r\}) = O(T_{\text{tr}}^2 r)$. Let K_{BCD} denote the number of block-coordinate descent iterations, which can be determined a priori in accord with Theorem 3.1. Then, the overall complexity of Algorithm 1 is $O(K_{\text{BCD}} T_{\text{tr}}^2 r)$.

The analysis above implies that the time complexity of a single iteration of Algorithm 3 is $O(K_{\text{BCD}} |\mathcal{D}|^2 T_{\text{tr}}^2 r)$. The time complexity of the soft-thresholding algorithm is $O(|\mathcal{D}|^2 T_{\text{tr}}^2 n)$. The training error bound given in Theorem 4.1 can be used to estimate a number of iterations needed to get the training error to within a pre-specified error bound. Let K_{AB} be the number of iterations of Algorithm 3 to be performed. The overall complexity of our proposed approach is then $O(K_{\text{AB}} K_{\text{BCD}} T_{\text{tr}}^2 r + |\mathcal{D}|^2 T_{\text{tr}}^2 n)$. In most cases, we will have that $r > n$ so that the total complexity can be simply be stated as $O(K_{\text{AB}} K_{\text{BCD}} T_{\text{tr}}^2 r)$. One can further reduce the computational complexity of Algorithm 1 by utilizing more efficient matrix multiplication and inversion techniques, our time complexity bounds assume standard matrix algebra techniques are used.

5 Experimental Results

Dataset and Network Description: We utilize a high-resolution dataset that was provided by the Abu Dhabi Department of Transportation. The dataset was obtained for Al Zahiyah in downtown Abu Dhabi and consists of the eleven intersections shown in Fig. 3. These intersections, currently operated by a commercial adaptive control tool, are the most congested in the city. For our experiments, we utilize data obtained from point sensors along the direction that is highlighted in the figure for three adjacent intersections. Each of the intersec-

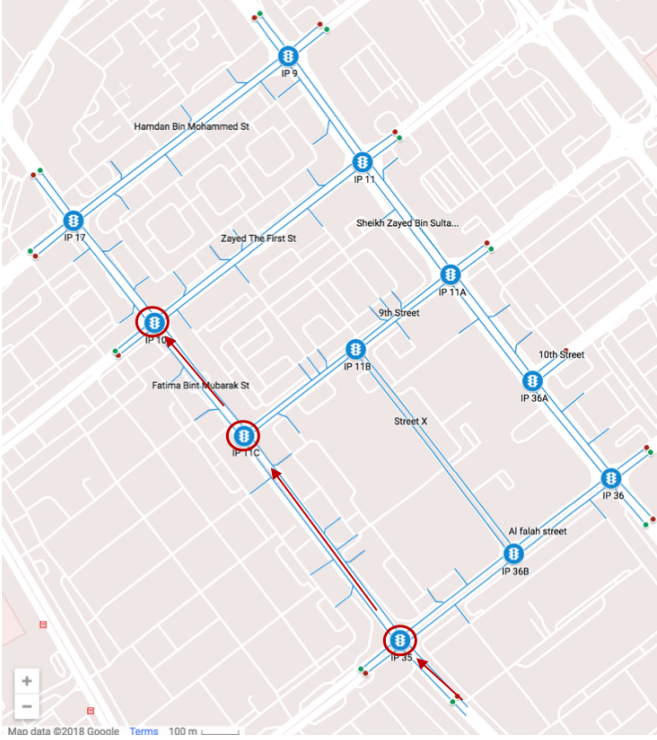


Figure 3: Layout of the Downtown Abu Dhabi Network.

tions has four through lanes in the northbound direction with one sensor in each lane. Each of the three intersections also has two left-turn lanes with sensor but we do not use these sensors for our experiments. Hence, the total number of sensors in our experiment is twelve. A schematic of one of the intersections is provided in Fig. 4. The sensors used are those in the advanced position (not the stop-line sensors).



Figure 4: A Schematic of One of the Intersections Used in the Experiment.

Description of Experiments: We test the proposed method using various horizons and lag times. Specifically, we test with $H \in \{1, 10, 60, 120\}$ and $L \in \{10, 30, 60, 120\}$ seconds. We use seven weeks of high-resolution data, 49 days, from the beginning of the first week of December, 2018 to the end of the third week of January, 2019. We do not distinguish workdays from weekends (as inputs) in our experiments as the proposed method is essentially a dynamic learning approach that is adaptive to time-varying changes and withing week patterns. The historical data used for boosting consists of $|\mathcal{D}| = 20$ consecutive days in each experiment. We benchmark our approach against the following prediction techniques:

1. Vector autoregressive time series (VAR): VAR models extend univariate autoregressive (AR) time series models to the vector case. This allows VAR models to capture correlations between different univariate time series. VAR models have been widely applied in forecasting multivariate traffic data.
2. Support vector regression (SVR): SVR is the most popular form of support vector machines (SVMs) and it has been applied in various fields, i.e., time series prediction. In this experiment, we choose the basic SVR model with RBF kernels for comparison.

3. Recurrent neural networks (RNN): RNNs are powerful tools for time series. In our experiments, we employ a long short-term memory (LSTM) architecture [12] with four layers (input, LSTM layer, fully-connected layer and output).

Performance Metrics: We employ two performance metrics for comparison, the first is a traditional mean absolute error (MAE):

$$\epsilon_{\text{MAE}} = \frac{1}{nT_{\text{te}}} \sum_{t=1}^{T_{\text{te}}} \|\hat{\mathbf{y}}_{\text{te}}(t) - \mathbf{y}_{\text{te}}(t)\|_1, \quad (124)$$

where $\hat{\mathbf{y}}_{\text{te}}(t)$ and $\mathbf{y}_{\text{te}}(t)$ are columns $t \in \{1, \dots, T_{\text{te}}\}$ of $\hat{\mathbf{Y}}_{\text{te}}$ and \mathbf{Y}_{te} , respectively. The second metric is the Skorokhod M_1 metric:

$$d_{M_1}(\hat{\mathbf{Y}}_{\text{te}}, \mathbf{Y}_{\text{te}}) \equiv \inf_{\substack{(\hat{Y}, \hat{y}) \in \Pi(\hat{\mathbf{Y}}_{\text{te}}), \\ (Y, y) \in \Pi(\mathbf{Y}_{\text{te}})}} \max \{ \|\hat{Y} - Y\|_{\infty}, \|\hat{y} - y\|_{\infty} \}, \quad (125)$$

where $\|\cdot\|_{\infty}$ is the uniform norm and $\Pi(\mathbf{Y})$ is the set of parametric representations of the rows of \mathbf{Y} . The Skorokhod M_1 metric is a particularly suitable metric for processes with jumps, more specifically, it allows for comparisons between processes with jumps and those free of jumps. We refer to [53] for a more detailed description of the metric. In our context, it is chosen for its ability to compare high-resolution signals. Finally, all the tests are run on a 2.7 GHz intel Core i7 Processor with 16 GB of RAM.

Impact of Choice of Lag and Horizon: Our results are summarized in Table 1 for the three intersections in the experiment at using various lags $L \in \{10, 30, 60, 120\}$ seconds and for different prediction horizons $H \in \{1, 10, 60, 120\}$ seconds into the future. Since all entries in both $\hat{\mathbf{Y}}_{\text{te}}$ and \mathbf{Y}_{te} are binary, we have that $\epsilon_{\text{MAE}} \in [0, 1]$ and $d_{\text{MAE}}(\hat{\mathbf{Y}}_{\text{te}}, \mathbf{Y}_{\text{te}}) \in [0, 1]$. We can hence measure accuracy using $1 - \epsilon_{\text{MAE}}$ and $1 - d_{\text{MAE}}$, where we have drop the arguments from the latter where no confusion may arise. The highlighted entries are those with the highest accuracies for each prediction horizon. The overall testing accuracy is no lower than 78.98% and reaches 91.07%. As expected, the accuracies tend to decrease as H gets larger. However, increasing the

lag L is not observed to improve the accuracy, a lag of $L = 30$ seconds seems to be the best choice in our experiment.

Table 1: Testing Accuracy of Proposed Algorithm's Prediction ($1 - \epsilon_{\text{MAE}}$).

Intersection 1				
$ \mathcal{D} \times L$	$H = 1$	$H = 10$	$H = 60$	$H = 120$
20×10	0.8908	0.8691	0.8505	0.8108
20×30	0.9107	0.8906	0.8515	0.8357
20×60	0.8759	0.8517	0.8218	0.8115
20×120	0.8515	0.8275	0.8115	0.7898

Intersection 2				
$ \mathcal{D} \times L$	$H = 1$	$H = 10$	$H = 60$	$H = 120$
20×10	0.9055	0.8850	0.8410	0.7798
20×30	0.9213	0.9050	0.8515	0.8275
20×60	0.8718	0.8405	0.8158	0.7608
20×120	0.8458	0.8128	0.7905	0.7595

Intersection 3				
$ \mathcal{D} \times L$	$H = 1$	$H = 10$	$H = 60$	$H = 120$
20×10	0.8838	0.8688	0.8570	0.8215
20×30	0.8990	0.8719	0.8584	0.8370
20×60	0.8815	0.8680	0.8358	0.8389
20×120	0.8617	0.8425	0.8318	0.8109

We see the same patten when measuring accuracy using $1 - d_{M_1}$. We illustrate this in Table 2 and Fig. 5 for the $L = 30$ seconds. This indicates that the general pattern (the overall trajectory observed at the sensors) was predicted with reasonable accuracy. An example of two signals, ground truth vs predicted for a randomly chosen sensor over a 100 second period during the morning peak, is given in Fig. 6.

Choice of Rank Parameter, r : We next investigate the performance of our approach for different choices of the input r in (25) and (28). We do so for the case $L = 30$ and $H = 10$ seconds. The objective values achieved when the algorithm converges for different values of r are depicted in Fig. 7. We

Table 2: Testing Accuracy of Proposed Algorithm's Prediction Using the Skorokhod M_1 Metric ($1 - d_{M_1}$).

H (sec)	Int. 1	Int. 2	Int. 3	Mean
1	0.8756	0.9109	0.8563	0.8809
10	0.8704	0.8865	0.8635	0.8734
60	0.8379	0.8603	0.8519	0.8500
120	0.8315	0.8285	0.8390	0.8330

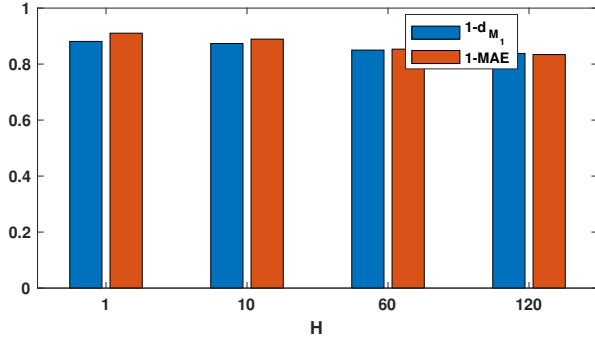


Figure 5: Prediction Performance for Different Horizons H .

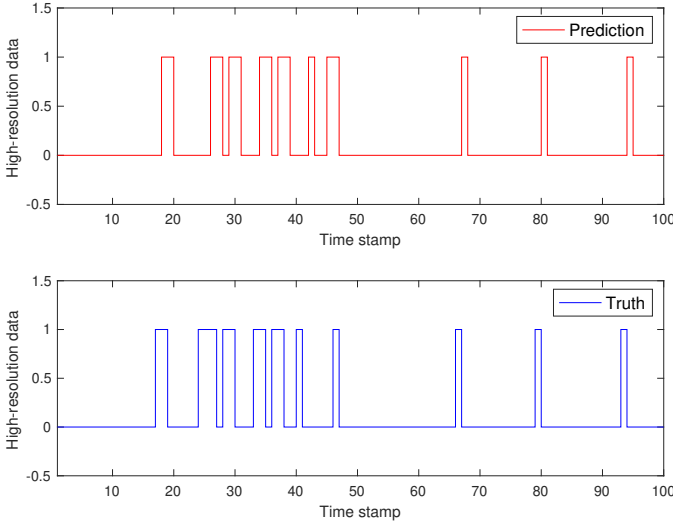


Figure 6: Example Sensor Signal Comparison, $H = 10$ seconds.

see that the lowest objective value is achieved when $r = 30$ indicating a highly sparse matrix (an order of magnitude smaller than both $nh \sim |\mathcal{D}|Ln$ and $|\mathcal{D}|T_{tr} + T_{te}$). Figures 8 and 9 Illustrate the sub-linear convergence rate of the algorithm for same

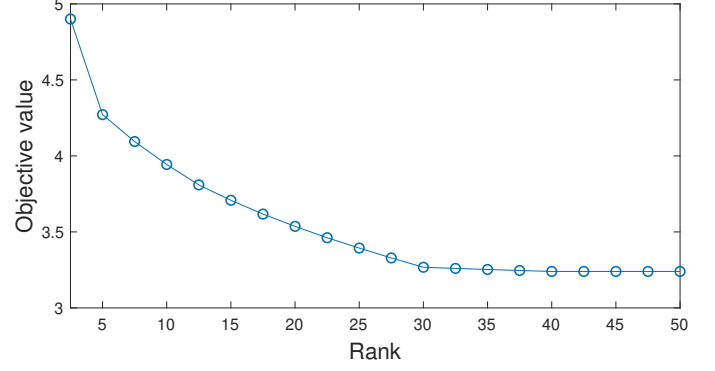


Figure 7: Relationship Between $r \geq \text{rank}(\hat{\mathbf{Z}})$ and Objective Function Value at Convergence.

experiment.

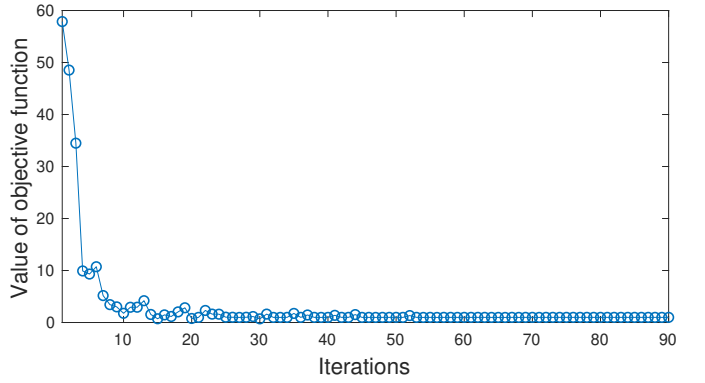


Figure 8: Convergence Rate.

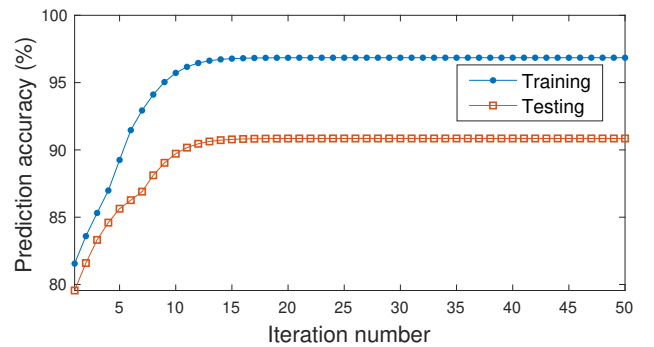


Figure 9: Illustration of Sub-Linear Convergence Rate.

Comparisons: We now show the results of our comparisons. In addition to VAR, SVR, and RNN, we perform comparisons against matrix completion with boosting (BMC) and without boosting. The

accuracy results are summarized in Table 3. We first note the improved performance with boosting. Next we notice that BMC outperforms both SVR and VAR and has comparable performance to the RNN, but unlike the RNN, the results are easy to interpret. We also provide a visual comparison il-

Table 3: Accuracy Comparisons

Method	$1 - d_{M_1}$	$1 - \epsilon_{MAE}$
MC	0.8105	0.8674
BMC	0.8809	0.9103
VAR	NAN	0.8014
SVR	0.7805	0.8669
RNN	0.8753	0.9151

lustrating the predicted sensor states for two sensors over a 100 second period in Fig. 10; the two sensors are located at two different intersections (intersection 2 and intersection 3). The bottom row in each sub-figure is the ground truth signal. For the first sensor, both BMC and the RNN capture the true patterns and both outperform the other methods. For sensor 3, BMC has the best performance. In both cases, VAR (the classical approach) performed poorly. This is to be expected for high-resolution data as VARs tend to smooth data (cf. the duality of auto-regression and moving averages), which precludes their ability to capture spikes in the process.

6 Conclusions

Our contribution can broadly be described as specializing contemporary convex optimization techniques to traffic prediction. These techniques have revolutionized a variety of applications that involve large volumes of data, from image processing to online recommender systems. However, they seem to have found little or no application in transportation science and traffic management. Our analysis demonstrates that one can solve large prediction problems in real-time (sub-linear convergence rate) and that the solutions obtained are block coordinate-wise minimizers. We also demonstrated that training error can be made arbitrarily small with ensemble learning. The latter are typically used to amalgamate results from heteroge-

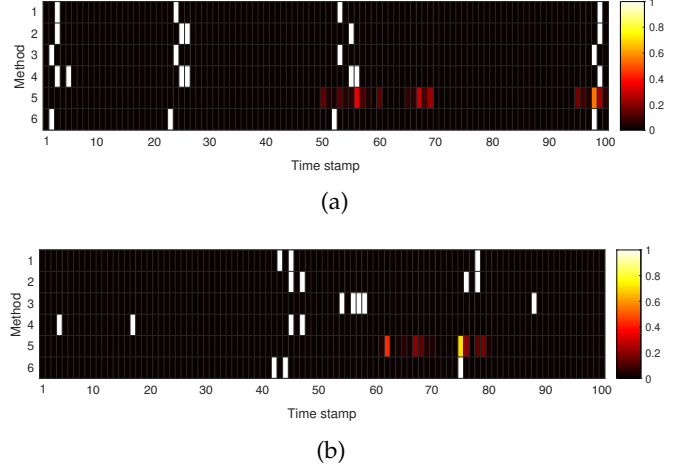


Figure 10: Example Signal Comparisons (a) A Sensor Along Intersection 1 and (b) A Sensor Along Intersection 3. (Methods: 1 = BMC, 2 = MC, 3 = RNN, 4 = SVR, 5 = VAR, 6 = Ground Truth)

neous techniques. Our implementation uses historical data as predictors. We elected to perform ensemble learning in this way for the sake of interpretability of our results.

The analysis in this paper culminates in a bound on the training error. This result is a specialization of a well known bound that comes with the Adaboost algorithm. Our bound allows for any type of thresholding. Our results do not say anything about how these bounds generalize to testing errors but our empirical results suggest that the out-of-sample errors are similar to the training error, with difference that is less than 10%. Future work can be conducted along two separate lines: The first is generalization errors and bounds on out-of-sample errors. The second involves investigations of what should be considered an acceptable level of error. This will depend on the application; for example, for signal timing optimization a lag of three seconds in a sensor actuation forecast can trigger a signal status decision that results unwanted congestion. We leave these questions to future research.

Acknowledgment

This work was supported by the NYUAD Center for Interacting Urban Networks (CITIES), funded by Tamkeen under the NYUAD Research Institute

Award CG001 and by the Swiss Re Institute under the Quantum CitiesTM initiative. The authors would also like to acknowledge in-kind support received from the Abu Dhabi Department of Transportation, in the form of the high-resolution traffic data that were used in our experiments.

References

- [1] Amir Beck and Luba Tetruashvili, *On the convergence of block coordinate descent type methods*, SIAM journal on Optimization **23** (2013), no. 4, 2037–2060.
- [2] Emmanuel J Candès and Benjamin Recht, *Exact matrix completion via convex optimization*, Foundations of Computational Mathematics **9** (2009), no. 6, 717–772.
- [3] Emmanuel J. Candès and Terence Tao, *The power of convex relaxation: Near-optimal matrix completion*, IEEE Transactions on Information Theory **56** (2009), no. 5, 2053–2080.
- [4] Chenyi Chen, Jianming Hu, Qiang Meng, and Yi Zhang, *Short-time traffic flow prediction with ARIMA-GARCH model*, 2011 IEEE Intelligent Vehicles Symposium (IV), 2011, pp. 607–612.
- [5] Deepthi Dilip, Nikolaos Freris, and Saif Eddin Jabari, *Sparse estimation of travel time distributions using Gamma kernels*, Proceedings of the 96th Annual Meeting of the Transportation Research Board, Washington D.C., 2017, pp. No. 17–02971.
- [6] ———, *Systems and methods for sparse travel time estimation*, US Patent Application (2018), 15/893,524.
- [7] Yuguang Fang, Kenneth A Loparo, and Xi-angbo Feng, *Inequalities for the trace of matrix product*, IEEE Transactions on Automatic Control **39** (1994), no. 12, 2489–2490.
- [8] Yoav Freund and Robert E Schapire, *A decision-theoretic generalization of on-line learning and an application to boosting*, Journal of Computer and System Sciences **55** (1997), no. 1, 119–139.
- [9] Bidisha Ghosh, Biswajit Basu, and Margaret O’Mahony, *Multivariate short-term traffic flow forecasting using time-series analysis*, IEEE Transactions on Intelligent Transportation Systems **10** (2009), no. 2, 246–254.
- [10] Jianhua Guo, Billy M Williams, and Brian L Smith, *Data collection time intervals for stochastic short-term traffic flow forecasting*, Transportation Research Record **2024** (2007), no. 1, 18–26.
- [11] Frank E Harrell Jr, *Regression modeling strategies: with applications to linear models, logistic and ordinal regression, and survival analysis*, Springer International Publishing, Cham, Switzerland, 2015.
- [12] Sepp Hochreiter and Jürgen Schmidhuber, *Long short-term memory*, Neural Computation **9** (1997), no. 8, 1735–1780.
- [13] Jianming Hu, Pan Gao, Yunfei Yao, and Xudong Xie, *Traffic flow forecasting with particle swarm optimization and support vector regression*, 17th International IEEE Conference on Intelligent Transportation Systems (ITSC), 2014, pp. 2267–2268.
- [14] Sherif Ishak and Haitham Al-Deek, *Performance evaluation of short-term time-series traffic prediction model*, Journal of Transportation Engineering **128** (2002), no. 6, 490–498.
- [15] Saif Eddin Jabari, *A stochastic model of macroscopic traffic flow: Theoretical foundations*, Ph.D. Dissertation. The University of Minnesota Twin Cities, Minneapolis, MN, 2012.
- [16] Saif Eddin Jabari, Deepthi Dilip, DianChao Lin, and Bilal Thonnay Thodi, *Learning traffic flow dynamics using random fields*, IEEE Access **7** (2019), 130566–130577.
- [17] Saif Eddin Jabari, Nikolaos Freris, and Deepthi Dilip, *Sparse travel time estimation from streaming data*, Transportation Science (2019), (forthcoming).
- [18] Saif Eddin Jabari and Henry Liu, *A stochastic model of traffic flow: Theoretical foundations*, Transportation Research Part B: Methodological **46** (2012), no. 1, 156–174.

- [19] ———, *A stochastic model of traffic flow: Gaussian approximation and estimation*, Transportation Research Part B: Methodological **47** (2013), 15–41.
- [20] Prateek Jain, Praneeth Netrapalli, and Sujay Sanghavi, *Low-rank matrix completion using alternating minimization*, Proceedings of the 45th Annual ACM Symposium on Theory of Computing, 2013, pp. 665–674.
- [21] Young-Seon Jeong, Young-Ji Byon, Manoel Mendonca Castro-Neto, and Said M Easa, *Supervised weighting-online learning algorithm for short-term traffic flow prediction*, IEEE Transactions on Intelligent Transportation Systems **14** (2013), no. 4, 1700–1707.
- [22] Yiannis Kamarianakis and Poulicos Prastacos, *Forecasting traffic flow conditions in an urban network: Comparison of multivariate and univariate approaches*, Transportation Research Record **1857** (2003), no. 1, 74–84.
- [23] ———, *Space-time modeling of traffic flow*, Computers & Geosciences **31** (2005), no. 2, 119–133.
- [24] Yiannis Kamarianakis, Wei Shen, and Laura Wynter, *Real-time road traffic forecasting using regime-switching space-time models and adaptive LASSO*, Applied Stochastic Models in Business and Industry **28** (2012), no. 4, 297–315.
- [25] Danqing Kang, Yisheng Lv, and Yuan-yuan Chen, *Short-term traffic flow prediction with LSTM recurrent neural network*, Proceedings of the 20th IEEE International Conference on Intelligent Transportation Systems (ITSC), 2017, pp. 1–6.
- [26] Sung-Eun Kim and Debbie Niemeier, *A weighted autoregressive model to improve mobile emissions estimates for locations with spatial dependence*, Transportation Science **35** (2001), no. 4, 413–424.
- [27] S Vasantha Kumar and Lelitha Vanajakshi, *Short-term traffic flow prediction using seasonal ARIMA model with limited input data*, European Transport Research Review **7** (2015), no. 3, 21.
- [28] Semin Kwak and Nikolas Geroliminis, *Traffic forecasting for freeway networks by a localized linear regression time series model with a graph data dimensional reduction method*, Proceedings of the 19th Swiss Transport Research Conference, 2019, pp. 1–6.
- [29] Wenqing Li, Chunhui Zhao, and Furong Gao, *Linearity evaluation and variable subset partition based hierarchical process modeling and monitoring*, IEEE Transactions on Industrial Electronics **65** (2017), no. 3, 2683–2692.
- [30] Marco Lippi, Matteo Bertini, and Paolo Frasconi, *Short-term traffic flow forecasting: An experimental comparison of time-series analysis and supervised learning*, IEEE Transactions on Intelligent Transportation Systems **14** (2013), no. 2, 871–882.
- [31] Henry X Liu, Wenteng Ma, Heng Hu, Xinkai Wu, and Guizhen Yu, *SMART-SIGNAL: Systematic monitoring of arterial road traffic signals*, 2008 11th International IEEE Conference on Intelligent Transportation Systems, 2008, pp. 1061–1066.
- [32] Yipeng Liu, Haifeng Zheng, Xinxin Feng, and Zhonghui Chen, *Short-term traffic flow prediction with Conv-LSTM*, Proceedings of the 9th International Conference on Wireless Communications and Signal Processing (WCSP), 2017, pp. 1–6.
- [33] Jing Lu and Carolina Osorio, *A probabilistic traffic-theoretic network loading model suitable for large-scale network analysis*, Transportation Science **52** (2018), no. 6, 1509–1530.
- [34] Yisheng Lv, Yanjie Duan, Wenwen Kang, Zhengxi Li, and Fei-Yue Wang, *Traffic flow prediction with big data: A deep learning approach*, IEEE Transactions on Intelligent Transportation Systems **16** (2014), no. 2, 865–873.
- [35] Xiaolei Ma, Zhuang Dai, Zhengbing He, Jihui Ma, Yong Wang, and Yunpeng Wang, *Learning traffic as images: A deep convolutional neural network for large-scale transportation network speed prediction*, Sensors **17** (2017), no. 4, 818.

- [36] Xiaolei Ma, Zhimin Tao, Yinhai Wang, Haiyang Yu, and Yunpeng Wang, *Long short-term memory neural network for traffic speed prediction using remote microwave sensor data*, Transportation Research Part C: Emerging Technologies **54** (2015), 187–197.
- [37] Andrew L Maas, Awni Y Hannun, and Andrew Y Ng, *Rectifier nonlinearities improve neural network acoustic models*, Proceedings of the 30th International Conference on Machine Learning, vol. 28, 2013, pp. 1–6.
- [38] Jonathan Mackenzie, John F Roddick, and Rocco Zito, *An evaluation of HTM and LSTM for short-term arterial traffic flow prediction*, IEEE Transactions on Intelligent Transportation Systems **20** (2018), no. 5, 1847–1857.
- [39] Cheol Oh, Stephen G Ritchie, and Jun-Seok Oh, *Exploring the relationship between data aggregation and predictability to provide better predictive traffic information*, Transportation Research Record **1935** (2005), no. 1, 28–36.
- [40] Carolina Osorio and Gunnar Flötteröd, *Capturing dependency among link boundaries in a stochastic dynamic network loading model*, Transportation Science **49** (2014), no. 2, 420–431.
- [41] Carolina Osorio and Vincenzo Punzo, *Efficient calibration of microscopic car-following models for large-scale stochastic network simulators*, Transportation Research Part B: Methodological **119** (2019), 156–173.
- [42] Mohsen Ramezani, Jack Haddad, and Nikolas Geroliminis, *Dynamics of heterogeneity in urban networks: aggregated traffic modeling and hierarchical control*, Transportation Research Part B: Methodological **74** (2015), 1–19.
- [43] Benjamin Recht, Maryam Fazel, and Pablo A Parrilo, *Guaranteed minimum-rank solutions of linear matrix equations via nuclear norm minimization*, SIAM Review **52** (2010), no. 3, 471–501.
- [44] T. Seo, A. Bayen, T. Kusakabe, and Y. Asakura, *Traffic state estimation on highway: A comprehensive survey*, Annual Reviews in Control **43** (2017), 128–151.
- [45] Alex J Smola and Bernhard Schölkopf, *A tutorial on support vector regression*, Statistics and Computing **14** (2004), no. 3, 199–222.
- [46] James H Stock and Mark W Watson, *Vector autoregressions*, Journal of Economic Perspectives **15** (2001), no. 4, 101–115.
- [47] Lu Sun, *Stochastic projection-factorizing method based on piecewise stationary renewal processes for mid-and long-term traffic flow modeling and forecasting*, Transportation Science **50** (2015), no. 3, 998–1015.
- [48] Johan AK Suykens and Joos Vandewalle, *Least squares support vector machine classifiers*, Neural Processing Letters **9** (1999), no. 3, 293–300.
- [49] Huachun Tan, Yuankai Wu, Bin Shen, Peter J Jin, and Bin Ran, *Short-term traffic prediction based on dynamic tensor completion*, IEEE Transactions on Intelligent Transportation Systems **17** (2016), no. 8, 2123–2133.
- [50] National Research Council Transportation Research Board, *Highway capacity manual*, Transportation Research Board, Washington, DC, 2000.
- [51] Eleni Vlahogianni and Matthew Karlaftis, *Temporal aggregation in traffic data: Implications for statistical characteristics and model choice*, Transportation Letters **3** (2011), no. 1, 37–49.
- [52] Wenyi Wang and Albert K Wong, *Autoregressive model-based gear fault diagnosis*, Journal of Vibration and Acoustics **124** (2002), no. 2, 172–179.
- [53] Ward Whitt, *Stochastic-process limits: An introduction to stochastic-process limits and their application to queues*, Springer-Verlag, New York, NY, 2002.
- [54] Billy M Williams and Lester A Hoel, *Modeling and forecasting vehicular traffic flow as a seasonal ARIMA process: Theoretical basis and empirical results*, Journal of Transportation Engineering **129** (2003), no. 6, 664–672.

- [55] Chun-Hsin Wu, Jan-Ming Ho, and Der-Tsai Lee, *Travel-time prediction with support vector regression*, IEEE Transactions on Intelligent Transportation Systems **5** (2004), no. 4, 276–281.
- [56] Yangyang Xu and Wotao Yin, *A block coordinate descent method for regularized multiconvex optimization with applications to nonnegative tensor factorization and completion*, SIAM Journal on Imaging Sciences **6** (2013), no. 3, 1758–1789.
- [57] Mehmet Yildirimoglu and Nikolas Geroliminis, *Experienced travel time prediction for congested freeways*, Transportation Research Part B: Methodological **53** (2013), 45–63.
- [58] Guohui Zhang and Yinhai Wang, *A gaussian kernel-based approach for modeling vehicle headway distributions*, Transportation Science **48** (2013), no. 2, 206–216.
- [59] Fangfang Zheng, Saif Eddin Jabari, Henry Liu, and DianChao Lin, *Traffic state estimation using stochastic Lagrangian dynamics*, Transportation Research Part B: Methodological **115** (2018), 143–165.